FACULTY OF PSYCHOLOGY AND EDUCATIONAL SCIENCES

Slave to the rhythm: Behavioral Consequences of Neuronal Oscillations

A Computational Modeling Approach

Word count: 10,327

Rien Sonck
Student number: 01402685

Supervisor(s): Dr. Mehdi Senoussi, Prof. Dr. Tom Verguts

A dissertation submitted to Ghent University in partial fulfillment of the requirements for the degree of Master of Science in Experimental and Theoretical Psychology

Academic year: 2019 – 2020

GHENT UNIVERSITY

Preamble concerning COVID-19

The COVID-19 pandemic did not cause any implications for this dissertation.

Preface

I want to thank Prof. Dr. Tom Verguts for introducing me to computational modeling and giving me the opportunity to learn from him. I also want to thank Dr. Mehdi Senoussi. Working together with him was a fun and great learning experience; through him, I was able to improve my programming, analytical, and writing skills.

In my six years at the University of Ghent, my grandparents have always stood beside me. They took care of me and always provided me with a place to study. They believed in me and supported me. Unfortunately, my grandmother passed away due to cancer on the 28th of July. Before she passed away, I promised her to dedicate my thesis to her.

Meter Enna,

I dedicate this one to you.

For all the love and support you have given me.

You always were and always will be our Sunshine.

You will be dearly missed.

Loves,

Rien

Abstract

Theta oscillations (between 4 and 7Hz) play a central role in cognitive control but, it remains unclear how the specific frequency of these oscillations affects cognitive control processes and if it can explain inter-individual variability in performance observed in cognitive control tasks. To investigate this, we used a computational model of cognitive control (i.e., the sync-model, Verguts's (2017)) and performed a qualitative model analysis where we explored the model's parameter space. Next, we performed a quantitative model analysis, where we conducted a parameter recovery analysis and fitted the model to empirical data. The qualitative analysis showed that the model's theta-band frequencies affect cognitive control and lead to inter-individual variability while the qualitative analysis was less conclusive. The sync-model allowed us to model and analyze how neural oscillations result in cognitive control and showed us that it is possible to fit the sync-model to empirical data to extract key parameters.

Keywords: cognitive control, theta oscillations, computational modeling

Table of Contents[i]

In everyday life we are faced with many different challenges throughout the day, some familiar such as making coffee in the morning and some new, never encountered before, such as finding a new route to work because the usual one is closed for roadworks. This ability to overcome habitual or automatic behavior in the face of external demands relies on what has been termed cognitive control. Cognitive control permits us to adapt behavior to external demands, crucial in an ever-changing environment. It allows us to (1) generate new goals (e.g., find a new route to work), (2) maintain our goals (e.g., keep searching for a new route until we find one), (3) suppress or inhibit irrelevant distractors (e.g., ignore the radio playing in our car), and (4) modify our selective attention based on our current goal (e.g., paying attention to the surrounding traffic) (Gratton et al., 2018). In the lab, cognitive control has classically been studied by using the Stroop task (Stroop, 1935). During the Stroop task, participants are presented with color words, see Figure 1. They have to name the ink color of the presented words. These words can be congruent or incongruent with the ink color. In congruent trials (Figure 1A) the ink color

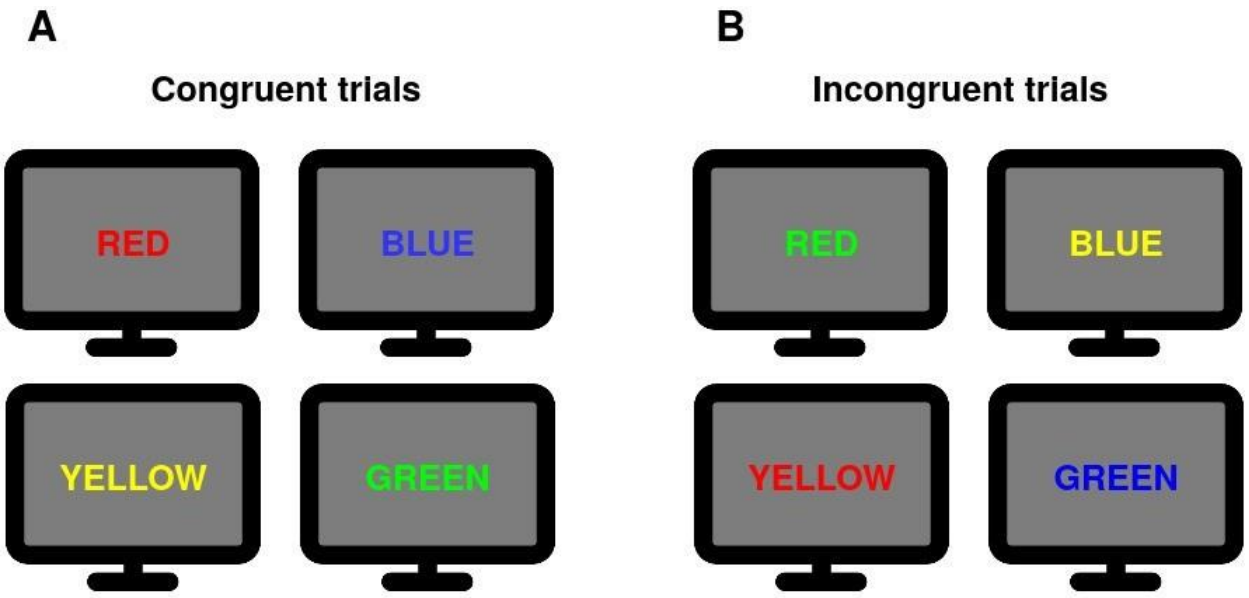

Figure 1. An example of stimuli that could be used in a Stroop task (Stroop, 1935). *Congruent trials contain words where the word matches the ink color of the word. Incongruent trials contain words where the word does not match the ink color of the word. Participants are slower in naming the ink color of words in the incongruent trials than in the congruent trials; this is coined the Stroop effect.*

and the word match (e.g., the word “Red” in red). In incongruent trials (Figure 1B) the ink color and the word do not match (e.g., the word “Red” in green). Stroop (1935) demonstrated that people have an automatic tendency to name the word and not the ink color. To name the ink color of a word in the incongruent trials, participants must overcome their habitual response by using cognitive control.

At the neural level, cognitive control is supported by a large network of brain areas such as the lateral prefrontal cortex (DLPFC), anterior cingulate cortex (dACC), and parietal cortex (DPC) (Breukelaar et al., 2017; Gratton et al., 2018; Miller & Cohen, 2001).

Furthermore, one mechanism has been shown to play a crucial role in cognitive control; neural oscillations, i.e. wave-like periodic modulations of neural activity, see Figure 2. More specifically when participants exert cognitive control in a particular task, neural oscillations have been observed in the medial frontal cortex (MFC) (Adam et al., 2020; Cavanagh & Frank, 2014; Gratton et al., 2018) in a specific band of frequencies (i.e., at a specific speed) called the theta frequency band (4 Hertz to 7 Hertz, i.e. a wave repeating 4 to 7 times per second), illustrated in Figure 3B. It is suggested that theta

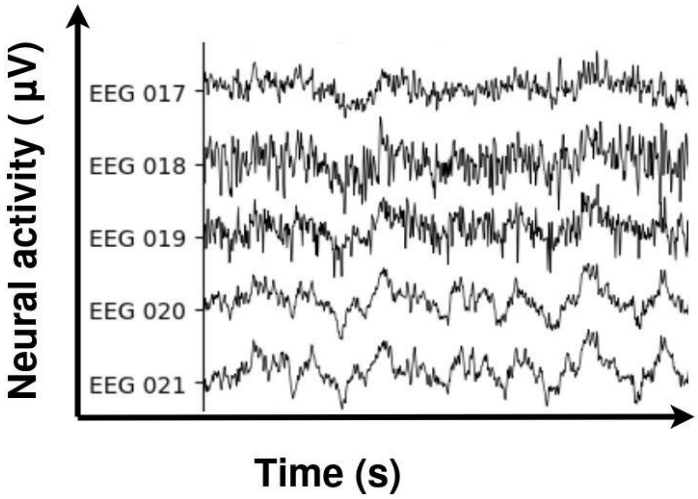

Figure 2. An example of neural oscillations in the brain. *Measured by an electroencephalogram (EEG), provided by the MNE python toolbox.*

oscillations generated by the MFC signal the implementation of cognitive control to adapt behavior in face of difficult, new, or changing task demands in the environment by synchronizing distant neural areas (Cavanagh & Frank, 2014; Gratton et al., 2018). The role of theta oscillations is thus central in cognitive control. However, the mechanistic implementation of cognitive control through theta oscillations is still unclear. It is essential to identify what aspects of theta oscillations affect cognitive control. In this study we focus

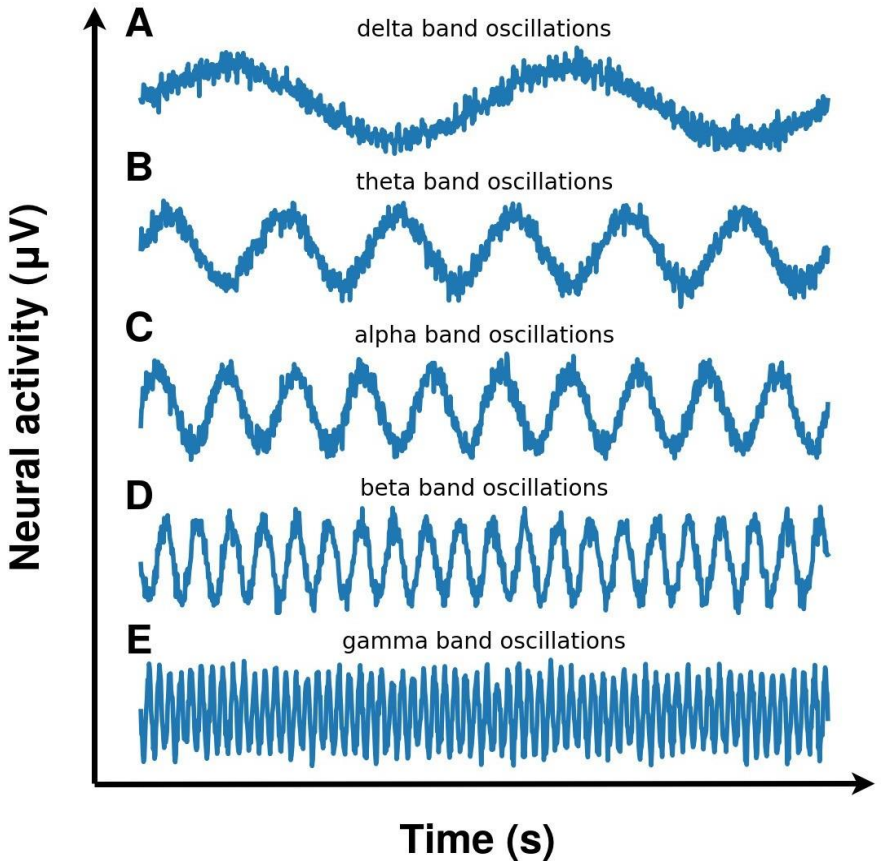

Figure 3. Frequency bands. *Neural oscillations are commonly functionally separated into different frequency bands (a range of frequencies):* **A.** *the delta band (between 1-4 Hz; 1-4 cycles per second),* **B.** *the theta band (between 4-8 Hz in humans and between 4-12 Hz in rats),* **C.** *the alpha band (between 8-12 Hz),* **D.** *the beta band (between 13-30 Hz), and E. the gamma band (between 30-200 Hz).*

on some pending questions about the link between theta oscillations and cognitive control.

(1) Theta oscillations can be described by their amplitude, frequency, and phase, see Figure 4. Many studies investigating the role of theta oscillations in cognitive control focused on band-average theta oscillation amplitudes, comparing the average amplitude in 4 to 7 Hz between conditions. It has been shown that theta band amplitude is

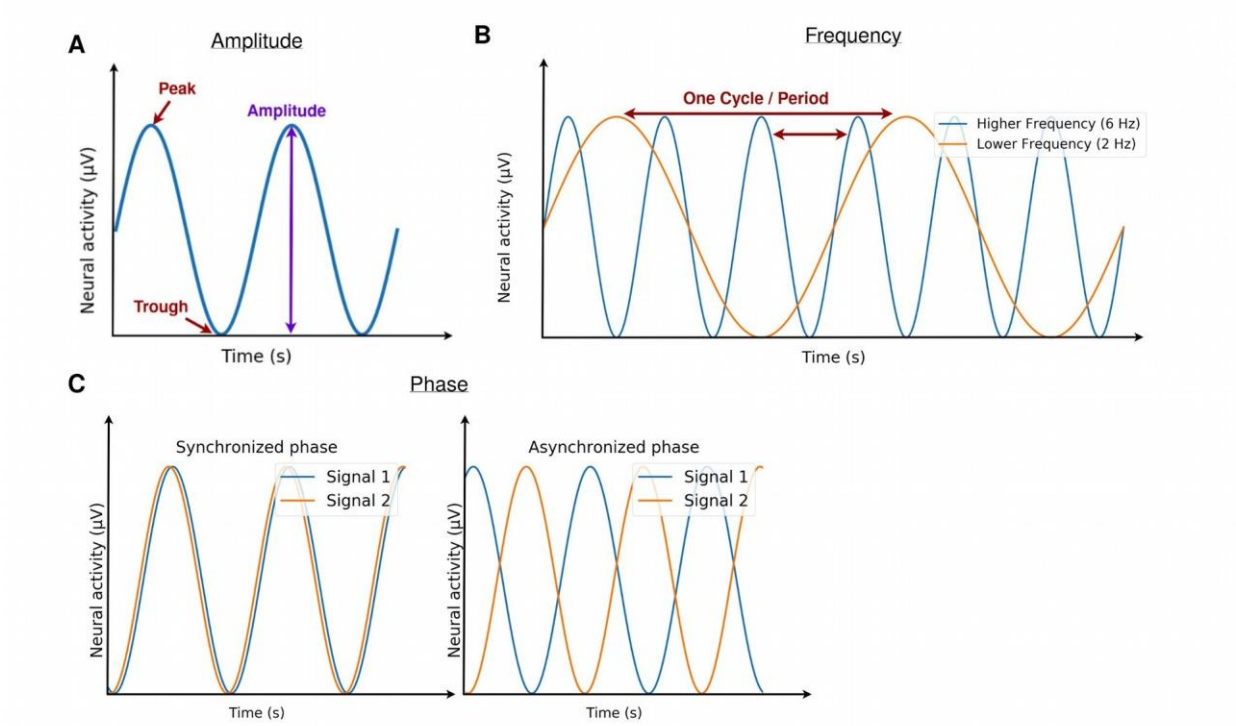

Figure 4. The characteristics of neural oscillations. *Neural oscillations are defined by their amplitude, frequency, and phase.* **A.** *The amplitude of neural oscillations represents the measure of the change in the electric signal.* **B.** *The frequency represents the number of repetitive waves (i.e. cycles) of neural activity that occur per unit of time. Commonly Hertz is used as a measure, indicating how many waves occur per 1 second.* **C.** *The phase is a measure to describe how two oscillating neuronal populations are occurring at the same time. Both populations can oscillate at the same frequency but the moment in time at which both populations their activity reaches a peak or trough might differ. When the peak and trough of two oscillating populations happen at the same moment in time, we can say that their phase is synchronized. When the peak and trough of two oscillations populations happen at different moments in time, we can say that their phase is asynchronized.*

modulated by task demands and that the amplitude is higher on successful trials (Cavanagh & Frank, 2014). But it remains unclear how specific theta frequencies are related to cognitive control. Does a frequency of 4 Hz affect cognitive control differently than a theta frequency of 6 Hz?

(2) If individual theta frequencies affect cognitive control it is also essential to understand if these vary across individuals. Can specific theta frequencies induce inter-individual variability, i.e., differences between individuals measured during a single task on a single occasion (MacDonald et al., 2006)? Inter-individual variability in cognitive control has been studied in the past (e.g., Eigsti et al., 2006; Gillie & Thayer, 2014; Holmes et al., 2016; Karayanidis et al., 2011; Lövdén et al., 2013) but it is still unclear what are the precise neural mechanisms that lead to inter-individual variability in cognitive control.

(3) It has been shown that theta oscillations have important interactions with other neural mechanisms, especially with higher frequency bands such as gamma oscillations (e.g., Axmacher et al., 2010; Bonnefond et al., 2017; Canolty et al., 2006; Colgin, 2016; Landau et al., 2015; Solomon et al., 2017). Theta oscillations are said to be temporal organizers for gamma frequencies (J. Lisman & Buzsaki, 2008; J. E. Lisman & Jensen, 2013; J. Lisman & Idiart, 1995). How does the interaction between theta oscillations and gamma oscillations affect cognitive control? And are there any other psychological mechanisms that interact with theta oscillations in supporting cognitive control?

To tackle these questions, we used a computational modeling approach. Building computational models is a fundamental tool of cognitive science research. They allow us to show computationally how cognition arises from neurobiological mechanisms. Furthermore, studying computational models that are capable of performing cognitive tasks has allowed us to understand many aspects of how cognition works and helped us to formulate new hypotheses, pushing the field of psychology and cognitive neuroscience forward (Kriegeskorte & Douglas, 2018).

In this study, we intend to better characterize how different aspects of theta oscillations affect cognitive control and whether this can explain inter-individual differences in task performance. To tackle these questions, we used a recent

computational model of cognitive control that relies on theta oscillations to implement cognitive control through synchronization of task-relevant units (sync-model, Verguts 2017). The sync-model uses neural oscillations to mechanistically achieve fast and flexible control of information processing across its different task modules (e.g., one module could be representing the color of the word in a Stroop task and another the response produced by the model). Due to its complexity, it has yet to be explored how different settings, e.g. the specific frequency of its theta oscillations, affect the model's behavioral performance in a specific task. In order to investigate the previously mentioned questions, we studied the sync-model parameters in function of their behavioral consequences: (1) the frequency of the MFC theta oscillations (i.e. MFC theta parameter), (2) the gamma variability parameter (to study the relationship between MFC theta and gamma oscillations), (3) the response threshold parameter (to investigate the relationship between MFC theta and other psychological mechanisms such as decision making). We utilized two main approaches: qualitative model analysis and quantitative model analysis. Both analysis approaches are in detail discussed in the methods section. We will first have a detailed look at the sync-model.

Computational model of cognitive control: sync-model

Verguts (2017) developed a computational model of cognitive control (sync-model). The sync-model implements cognitive control by using the principle "binding by random bursts" which utilizes neural networks to create task-relevant representation by using theta oscillations as a synchronizing mechanism. We will first explain the CTC theory, noise-induced synchronization, and binding by random bursts, then, we will demonstrate the sync-model on a Stroop task, to show how the sync-model works. Lastly, we will introduce the relevant parameters of the sync-model for this study.

Communication-through-coherence (CTC) theory. The CTC theory (Fries, 2005, 2015) is a theory on the mechanistic role of oscillations for neuronal communication between distant neuronal groups. Neuronal communication is the transfer of information (e.g., visual information that is used for adaptive behavior needs to be transferred to areas supporting decision-making and motor responses) from a sending (i.e., presynaptic) neuronal group to another receiving (i.e., postsynaptic) neuronal group.

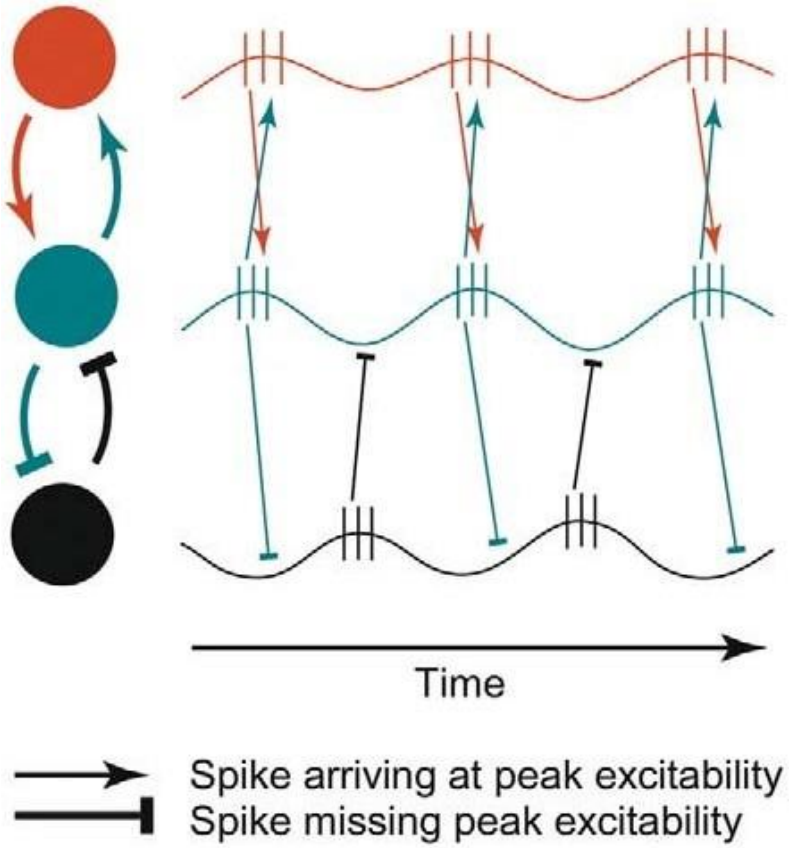

Figure 5. Example of the Communication-through-coherence from Fries (2015). *The arrows show information transfer (i.e., spike) sent between two neuronal groups that are phase synchronized. The spike from the red neuronal group arrives (with a small, fixed delay) at the excitability peaks of the receiving green neuronal group, thus their communication is effective. The blunt arrowheads show spikes that miss excitability peaks. The spikes sent from the black neuronal group miss the excitability peaks of the green neuronal group and therefore their communication is prohibited.*

It has been found that neural groups mostly oscillate between 30 Hz to 200 Hz, which is the gamma-frequency band (figure 3A) (Friedman-Hill, 2000; Fries et al. 2005, 1997; Fries et al., 2002; Gray et al., 1989; Maldonado, 2000). The CTC theory proposes that the neuronal communication between a sending and receiving neuronal group is more

effective, precise, and selective when the gamma oscillations of both neuronal groups are phase synchronized (illustrated in Figure 4C), which means that the oscillatory signals of both neuronal groups reach their peaks and throughs at the same time or with a fixed delay. Synchronization ensures that the information of the sending neuronal group arrives in a temporally organized manner at the receiving neuronal group, see Figure 5. The information also arrives while the receiving neuronal group is at a more excitable state,

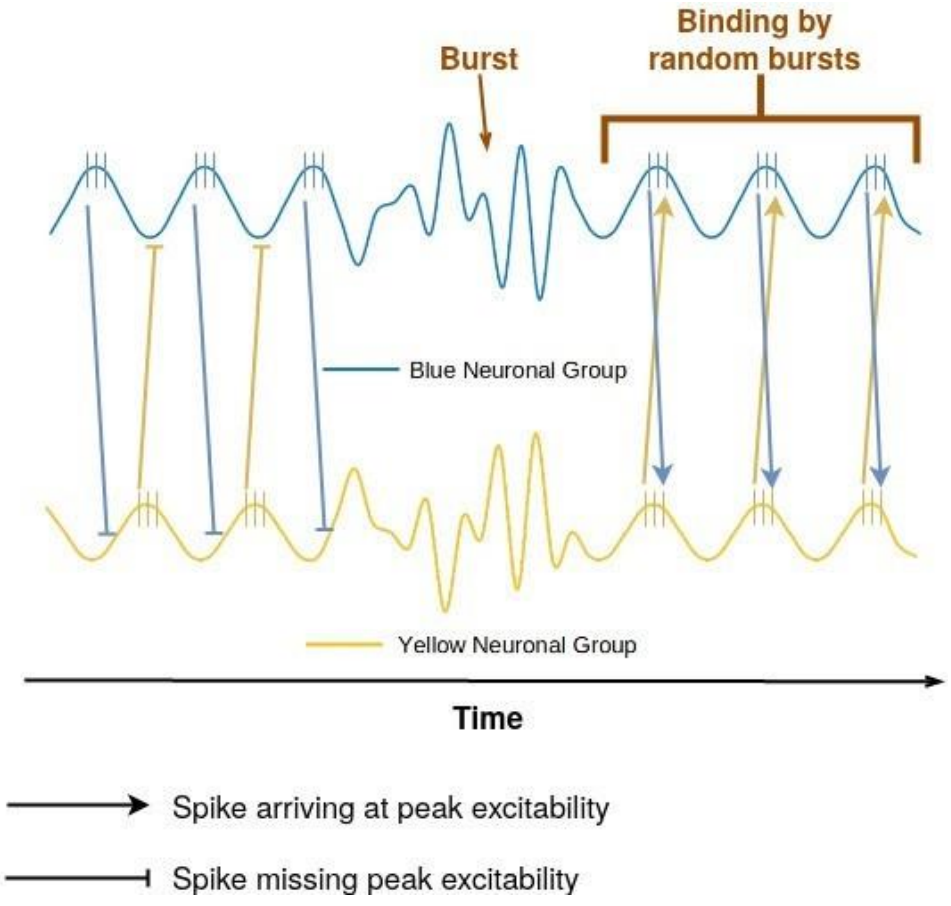

Figure 6. Example of binding by random bursts. *The blunt arrows show information (i.e., spikes) sent between the blue neuronal group and the yellow neuronal group. The spikes of both neuronal groups miss the peak excitability of each other and therefore their communication is prohibited. Next, an extracellular burst of noise arrives at both neuronal groups, phase-resetting them. The spikes sent by both neuronal populations now arrive at the peak excitability of each other, thus their communication is effective. The bursts bind both neuronal groups together.*

resulting in a higher probability to cause action potentials in the receiving neuronal group, therefore, increasing the probability of communicating this information to further areas. But how is synchronization induced between two neuronal groups to optimize their communication?

Noise-induced synchronization. Noise-induced synchronization (Zhou et al., 2005) explains how different oscillators (e.g., a pair of excitatory and inhibitory neurons generating oscillations together) can become phase-synchronized. An extracellular (i.e., outside of the neuron) disturbance of electrical activity (i.e., a burst of noise) hits a group of neurons. Only when the disturbance has passed, can these neurons pick-up their firing cycle again (which happens at the same time), thus phase synchronizing them.

Binding by random bursts. Binding by random bursts combines the CTC theory with noise-induced synchronization. Here, bursts of noise are sent to two neuronal groups, see Figure 6. Each burst phase-resets both neuronal groups, resulting in a higher probability that the information sent from one neuronal group will cause action potentials in the other neuronal group. This will eventually lead to both neuronal groups communicating effectively with each other.

Theta oscillations have been proposed to be able to reset the phase of two neuronal groups across the brain and forcing them to communicate (Bonnefond et al., 2017; Solomon et al., 2017; Voloh et al., 2015; Voloh & Womelsdorf, 2016).

A demonstration of the sync-model. Consider the following demonstration of the sync-model using a simplified Stroop Task (Stroop, 1935), see Figure 7. In this task, the rule is to press on the right key when the ink color of a word is green and to press on the left key when the ink color of a word is red. In the sync-model, the stimuli properties (e.g., the ink color of the word and the word itself) and the responses (e.g., left key press and a right key press) are represented by simplified cortical columns, see Figure 7B.

A cortical column is a group of local neurons that form a functional unit. This is coherent with the laminar cortical microcircuit structure of the neocortex (Douglas et al., 1989; Schroeder & Lakatos, 2009). Each cortical column consists of one rate code neuron and two-phase code neurons (one inhibitory and one excitatory). The rate code neurons receive, processes, and transmit information. Both phase code neurons act as

oscillators, their interaction generates gamma oscillations. These gamma oscillations coordinate when the rate code neurons transmit information to other rate code neurons.

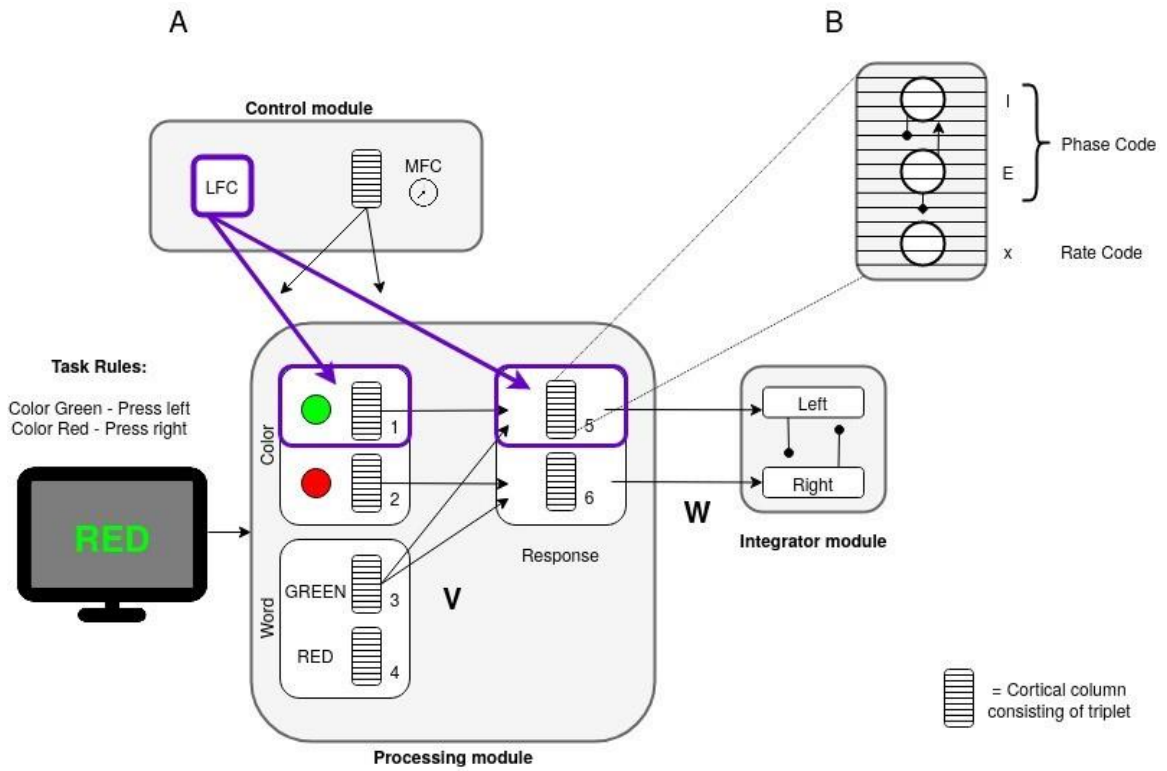

Figure 7. A graphic demonstration of the sync-model performing a simplified Stroop task (Stroop, 1935), this figure is adapted from Verguts (2017). **A.** *The word and the ink color (stimulus properties) and the left and right response (response options) are each represented by a cortical column (i.e. a unit). These units are in constant communication with each other. The control module implements cognitive control. The lateral frontal cortex (LFC) connects the task-relevant units; a green ink color is presented thus the task is to answer with a left key press. The LFC connects the sensory unit representing the green color and the response unit representing the left response. Next, the medial frontal cortex (MFC) generates theta oscillations and these theta oscillations emit noise bursts to both the LFC selected stimulus and response unit. These bursts of noise phase-resets the phase code neurons of these units (***B****), thus binding them together and making their communication effective. Information can now effectively be sent between both units their rate code neurons (****B****).*

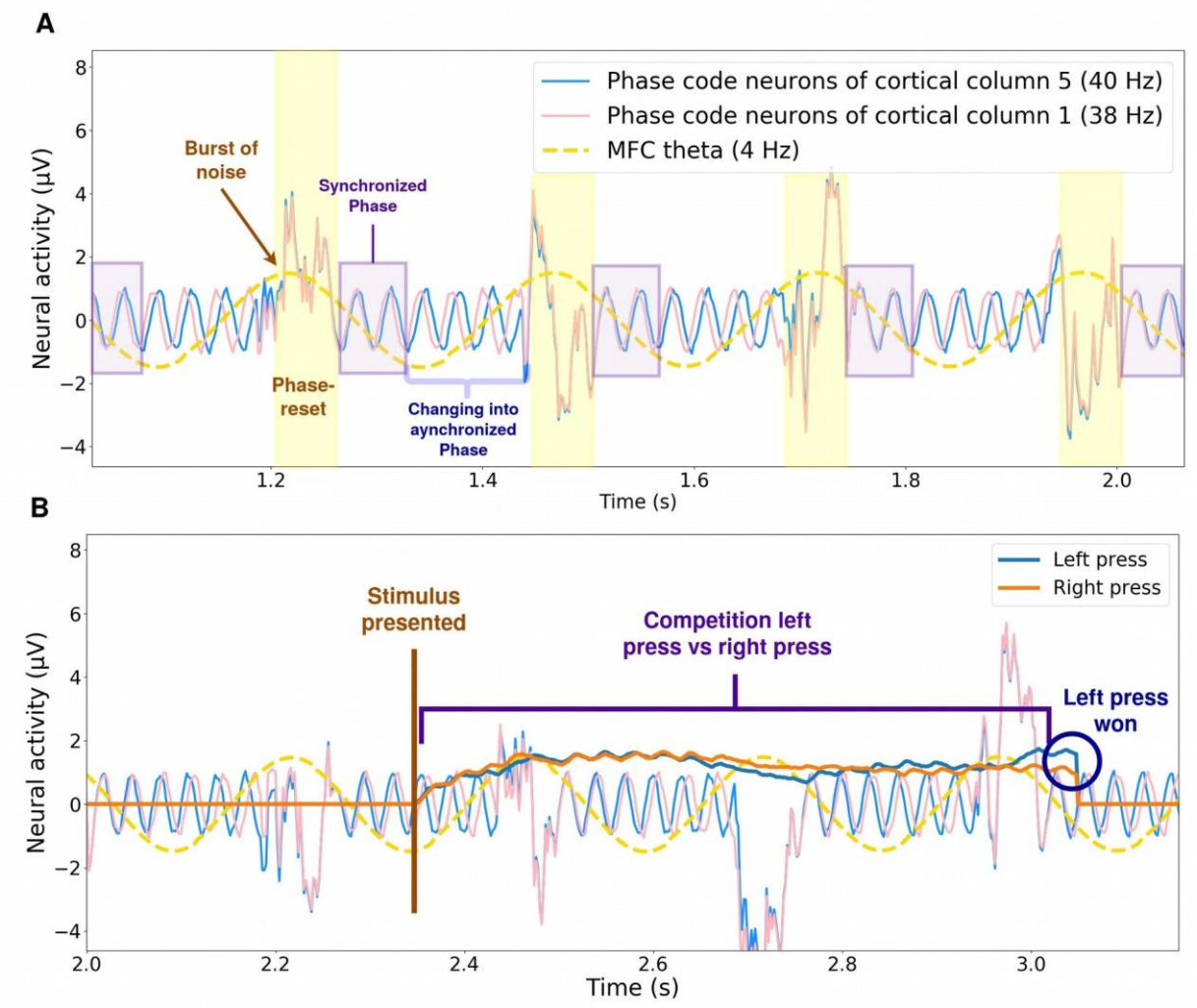

Figure 8. Illustration of the inner-workings of the sync-model performing a trial of the Stroop task depicted in Figure 7. **A.** *Both phase code neurons (one inhibitory and one excitatory) of each cortical column generate gamma oscillations. The medial frontal cortex (MFC) is generating theta oscillations at 4 Hz. These theta oscillations emit noise bursts in both cortical columns. Every time a burst emits, the phase code neurons of each cortical column phase-resets. This causes the gamma oscillations to phase synchronize, leading to a temporal window of effective communication. Because both gamma oscillations have a different frequency (38 Hz and 40 Hz) they do not stay phase synchronized. Across time their phase will become desynchronized, leading to an asynchronized phase between them.* **B.** *A trial starts, and a stimulus is presented (e.g. "RED" word in green ink color). The integrator modules integrate the information from the rate code neurons of the right and left response units. Competition starts between them. Because the left response unit is bound to a task-relevant sensory unit (e.g., green ink color), information is more effectively sent to the left response unit, thus the left response wins the competition.*

Let us consider a trial where the sync-model is presented with the word “RED” in green ink color, see Figure 7A. The control module contains the lateral frontal cortex (LFC) and medial frontal cortex (MFC), which together implement cognitive control.
On this current trial, the ink color is green, and the rule is to respond by giving a left key press. The LFC connects the cortical columns (i.e., units) that are relevant for completing this trial. Here, sensory unit 1 (green color) and response unit 5 (left press) are connected. Next, the MFC generates theta oscillations and through these theta oscillations, bursts are emitted to the LFC connected units. These bursts phase-synchronize the phase code neurons of both units, forcing them to eventually communicate effectively with each other, illustrated in Figure 8A. The interaction between the units in the processing module is then connected to an integrator module that allows producing model behavior. The integrator module is a competitive accumulator network (Usher & McClelland, 2001). The integrator modules integrate the information coming from response unit 5 (left response) and response unit 6 (right response), see Figure 8B. The left response unit and right response unit in the integrator module enter a competition, and if one of them exceeds a response threshold it wins this competition and gets selected as the response for the current trial. In the example depicted in Figure 8, response unit 5 is bound with the current relevant stimulus property (e.g., the green ink color; sensory unit 1) and the information sent towards the rate code neuron of response unit 5 is higher across time than the information sent to the rate code neuron of response unit 6.

MFC theta parameter. The MFC theta parameter defines the theta frequency of the MFC. The higher the theta frequency, the higher the number of noise bursts that are sent in a fixed period to task-relevant phase code neurons, because MFC theta oscillations reach their peak more frequently.

Gamma variability. The gamma variability parameter controls the difference in the precise gamma frequencies of cortical columns, e.g. if gamma variability is 2 the sensory units their gamma frequencies are at 38 Hz and the response units their gamma frequencies are at 40 Hz. The larger the difference between gamma oscillations of two units, the shorter their temporal window of phase synchronization will be.

Response threshold. The response threshold controls the amount of information that has to be accumulated by the integrator module before a response is

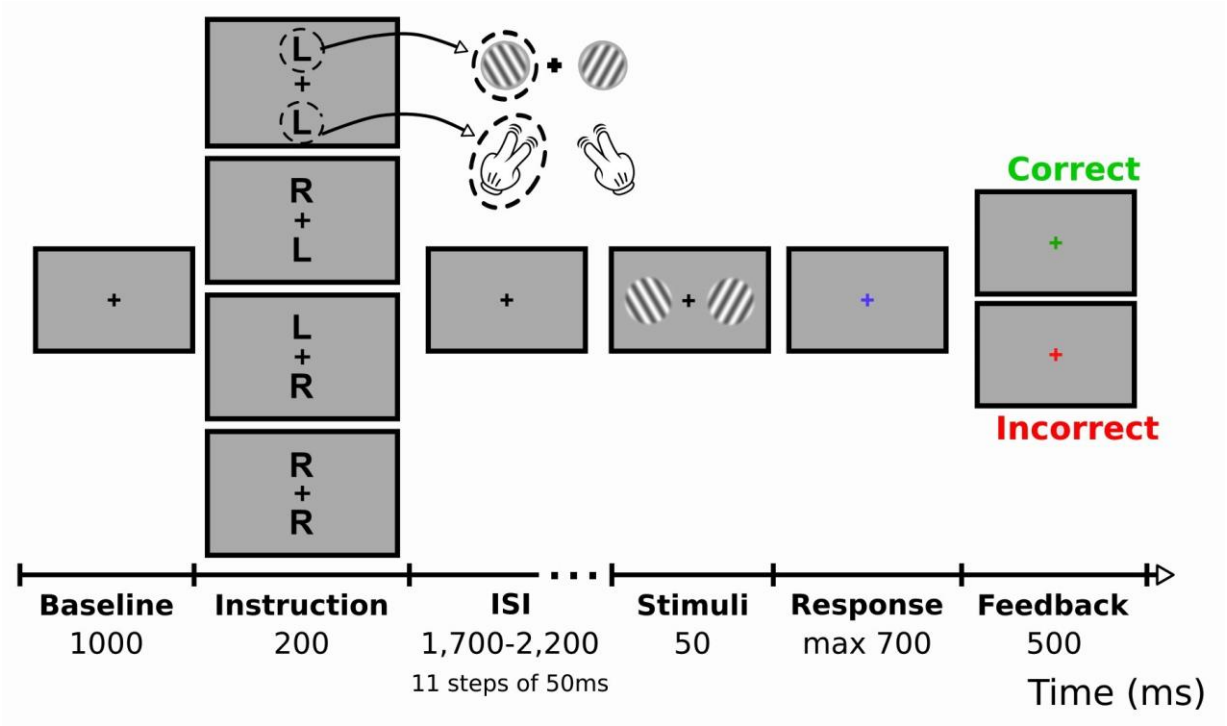

Figure 9. The 2-alternative forced-choice (2-AFC) orientation discrimination task from Senoussi et al. (2018). *The 2-AFC task is specially designed to study cognitive control due to participants having to quickly shift between different instructions. During the 2-AFC task, two letters are shown on the screen. The location of these letters (top vs bottom) and the letters themselves (L vs R) act as instructions. The top letter cues whether participants have to shift their attention towards the left or the right upcoming stimulus (L – left stimulus, R – right stimulus). The bottom letter cues which hand participants have to use to respond to this stimulus (L – left-hand, R – right-hand). These instructions were shown for 200m. Then, an interstimulus interval (ISI) followed. Across trials, the length of the ISI varied between 1700ms to 2200ms. Next, two sinusoidal gratings were simultaneously shown for 50ms, one appearing left on the screen and the other appearing right on the screen. Depending on the instructions, the participants shifted their attention to one of the gratings and prepared either their left-hand or right-hand to respond. Furthermore, the orientation of the attended grating (clockwise vs counterclockwise) signaled with which specific finger participants had to respond (index finger vs middle finger). They had a maximum of 700ms time to respond. After each trial, the feedback was given.*

produced by the model. The higher the response threshold, the more information has to be accumulated by one of the competing responses before it can win. This parameter can be seen as the cautiousness of the decision, if the threshold is high the model will need more information to trigger a response than if the threshold is low.

Methods

To understand how theta frequency affects performance and whether it can explain inter-individual differences in behavioral performance, we used two main approaches: qualitative model analysis and quantitative model analysis. The qualitative analysis permitted us to explore how different parameters affected model performance. The quantitative analysis was carried out to test whether specific model parameters allowed to fit the model to empirical data. This allowed us to check if the results from the qualitative model analysis are generalizable to empirical data. In order to carry out these approaches, we set up the sync-model to perform a stimulus-response mapping task to be able to compare model simulations to empirical data from Senoussi et al. (2018). The stimulus-response mapping task is illustrated in Figure 9. Electroencephalography (EEG) was also recorded during the task. The peak frequency of frontal theta oscillations was extracted in a 1s time window before the presentation of the stimuli. Thirty-four participants (18-32 years old; 25 females) performed the task. Importantly, adapting the model to perform the task from Senoussi et al. (2018) does not affect its core mechanisms. The only changes to the model compared to the Stroop task described above were the number of sensory and response units and which ones need to be synchronized to perform the task.

Qualitative analysis

Parameter space exploration. First, the sync-model was studied qualitatively. We explored the parameter space, which is the space (i.e., range) of possible values of each relevant sync-model parameter: the MFC theta, the gamma variability, and the response threshold. The values of each of these parameters can form the axes of a plot, and the behavioral performance on the stimulus-response mapping task for each given combination of the parameter values is plotted against these axes, see Figure 10. This can help us identify regions of the parameter space that behave differently (i.e., patterns).

For instance, do higher MFC theta frequencies lead to a different behavioral outcome than lower MFC theta frequencies? This approach is often used as a first step to reach a qualitative overview of how a model behaves across a different combination of its parameters (e.g., Steegen et al., 2017).

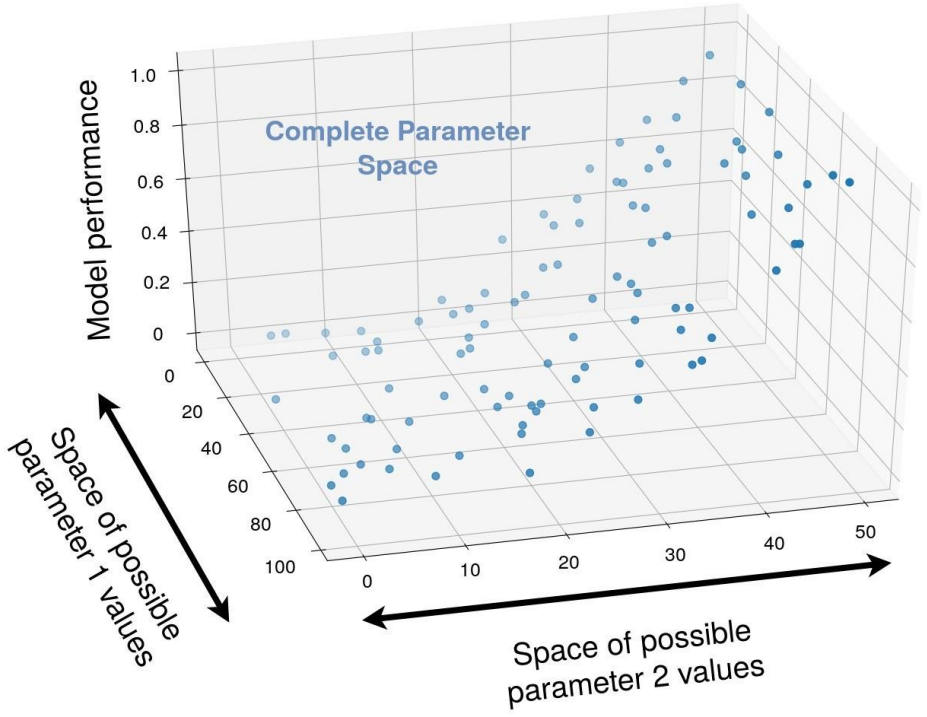

Figure 10. A toy example of parameter space exploration. *In this toy example, the parameter exploration allowed us to conclude that parameter 1 does not affect model performance.*

EZ-diffusion model (EDDM). In the stimulus-response mapping task behavioral performance was measured through response time (RT) and the probability of correct responses (Pc). The pitfall of only using these two measures to conduct a qualitative analysis is that the speed-accuracy trade-off might vary across parameters, e.g. some parameters leading to high accuracy but long response times and other parameters to the reverse relation (shorter response times but lower accuracy). This makes it challenging to compare parameters and to quantify which ones resulted in better task performance. To solve this, we used the EZ-diffusion model (EDDM) for two-choice response time tasks (Wagenmakers et al., 2007) to transform the mean RT (MRT), the

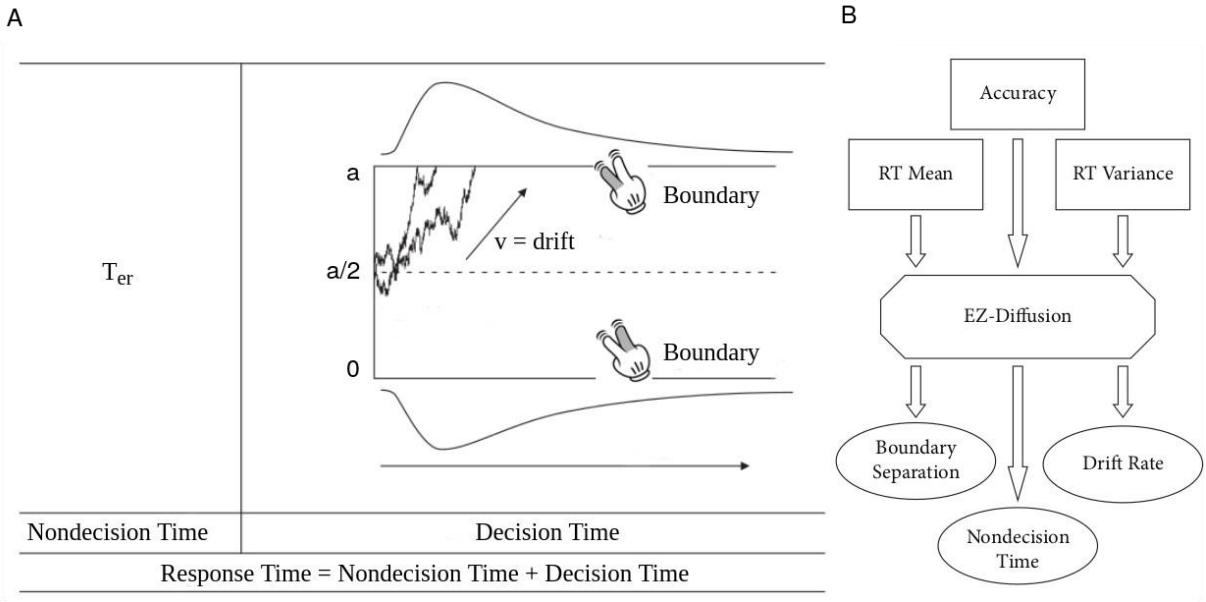

Figure 11. Illustration of the EZ-diffusion model (EDDM). **A.** T*he drift rate "v" represents the speed of information accumulation. When the accumulated information (i.e., evidence) by the drift rate "v" surpasses a threshold (i.e., boundary "a"), then the response associated with that threshold is given. The EDDM also captures the non-decision time component (T_{er}) of the response time.*

RT variance (VRT), and the Pc into three new unobserved variables of task performance: (1) drift rate "v" (i.e., the speed of information accumulation), (2) boundary separation "a" (i.e., how much information needs to be accumulated to reach a decision), and (3) T_{er} (i.e., non-decision time), see Figure 11B. These variables are assumed to underlie cognitive processes affecting the performance on the task, see Figure 11A. Using these three measures we were able to distinguish different aspects of the model's task performance.

Quantitative analysis

The quantitative analysis permitted us to investigate if the behavioral patterns identified by the qualitative analysis can be generalized to real participants. This will be done by fitting the sync-model parameters to empirical data from Senoussi et al. (2018). This allowed us to find values of the MFC theta, Gamma variability, and response

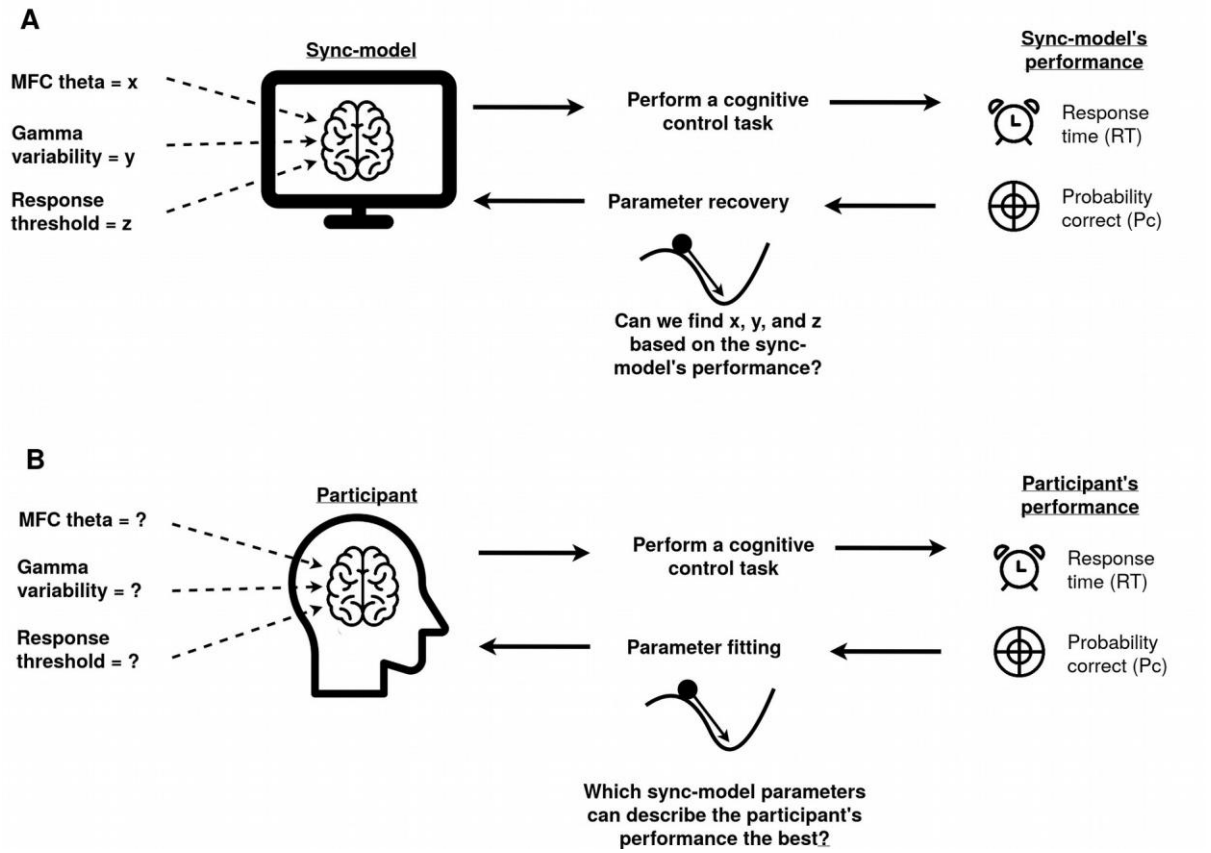

Figure 12. An illustration of the quantitative analysis step that we undertook. **A**. *The steps to complete a parameter recovery analysis. The sync-model's parameters are given a value; MFC theta is set to value x, gamma variability is set to value y, and the response threshold is set to value z. Next, the sync-model performs a cognitive task. This generates sync- model's behavioral performance (RT and Pc). This is used as our target data. The target data are given to a fitting function. This fitting function runs through different sets of sync- model parameters' values and generates new model behavioral data (i.e., simulated data) that match the target data best. Finally, the parameters' values of the best matching simulated data are compared to the parameters' values of the target data. If the recovered parameters' values are close to x, y, and z, then, the parameter recovery is successful.* **B.** *The steps to fit the sync-model to empirical data are the same as described in A. But now a participant's behavioral performance is our target data and we do not know the parameters' values of the target data. If the fitting function was successful in the parameter recovery analysis, then we should be able to "recover" correct participant parameters values.*

threshold that generate behavioral performance which can best describe (i.e., is closest to) the participant's performance. This is like linear regression, where we try to find the best regression coefficients for a given pattern of data. The steps we undertook in the quantitative analysis are illustrated in Figure 12.

Parameter recovery analysis. Before the sync-model can be fitted to participants' data, we need to ensure that the effects of its parameters are identifiable. Therefore, we carried out a "parameter recovery" analysis, see Figure 12A. First, the sync-model performs the stimulus-response mapping task with a known set of sync-model parameter values (e.g., MFC theta = 5, gamma variability = 3, response threshold = 3). This generates model behavioral performance on the task, summarized through the MRT and the Pc (which can be transformed into EDDM variables). This is used as our target data. Second, these target data are given to a fitting function. The fitting function runs through different sets of sync-model parameter values and attempts to generate new model behavioral data (i.e., simulated data) that match the target data best. To compare the simulated data to the target data the fitting function uses an error function, which measures how different the simulated data are from the target data. The fitting function uses a fitting algorithm to find a set of parameter values that minimizes the error function (i.e. difference between simulated data and target data). Once the fitting finished, we compared the recovered parameters' values to the ones we used to generate the target data to test whether these parameters were successfully recovered.

The error function is developed based on the results of the qualitative analysis. This helps to find behavioral patterns that can best dissociate between different parameter values. For instance, a fast RT is associated with a higher MFC theta value, thus the error function could use the RT in the error function to allow the fitting algorithm to dissociate between MFC theta values.

Participant fitting. Once we ensured that parameter recovery is possible on model data, we used this fitting procedure to fit the sync-model parameters to empirical data, as illustrated in Figure 12B. Instead of using data generated by the sync-model itself, the participants' behavioral data are now used as the target data. The fitting function tries to find sync-model parameters' values that generate a model behavioral performance that most closely resembles the participants' performance.

Once the sync-model parameters were fitted to a range of participants, these fitted parameters can be used to study if the behavioral patterns found in the qualitative analysis of the model's behavioral performance (e.g., higher theta frequency leads to higher model performance), which can be considered as predictions of the model, are validated by empirical data.

Software

The sync-model was written in Python (v3.7.7, van Rossum, 1995). All analyses were carried out in either Python or R (v3.6.2., The R Foundation for Statistical Computing)

Results

To summarize, first, a qualitative analysis was performed. This includes a parameter space exploration. Next, a quantitative analysis was conducted, which consisted of a model's parameter recovery analysis and fitting the model to empirical data.

Qualitative analysis: parameter space exploration

The parameter space exploration was conducted by running 276 sync-model simulations on the stimulus-response mapping task. During each simulation, 880 trials were performed, resulting in a total of 242 880 trials. The MFC theta, gamma variability, and response threshold were varied across the simulations.

Gamma variability. The gamma variability was varied between values of 1 Hz and 5 Hz. Setting the gamma variability to 1 Hz sets the gamma frequency at 38 Hz for sensory units and 39 Hz for the response units. Setting the gamma variability to 5 Hz sets the gamma frequency of the sensory units to 38 Hz and those of the response units to 43 Hz. The average gamma frequency across simulations was around 40 Hz. Units that had gamma frequencies that were closer (i.e. low gamma variability) phase-synchronized for longer, as demonstrated in Figure 13A-B. The amount of time that two cortical columns can stay phase-synchronized is reflected in the behavioral performance, see Figure 14. The larger the gamma variability, the worse the performance on all the performance

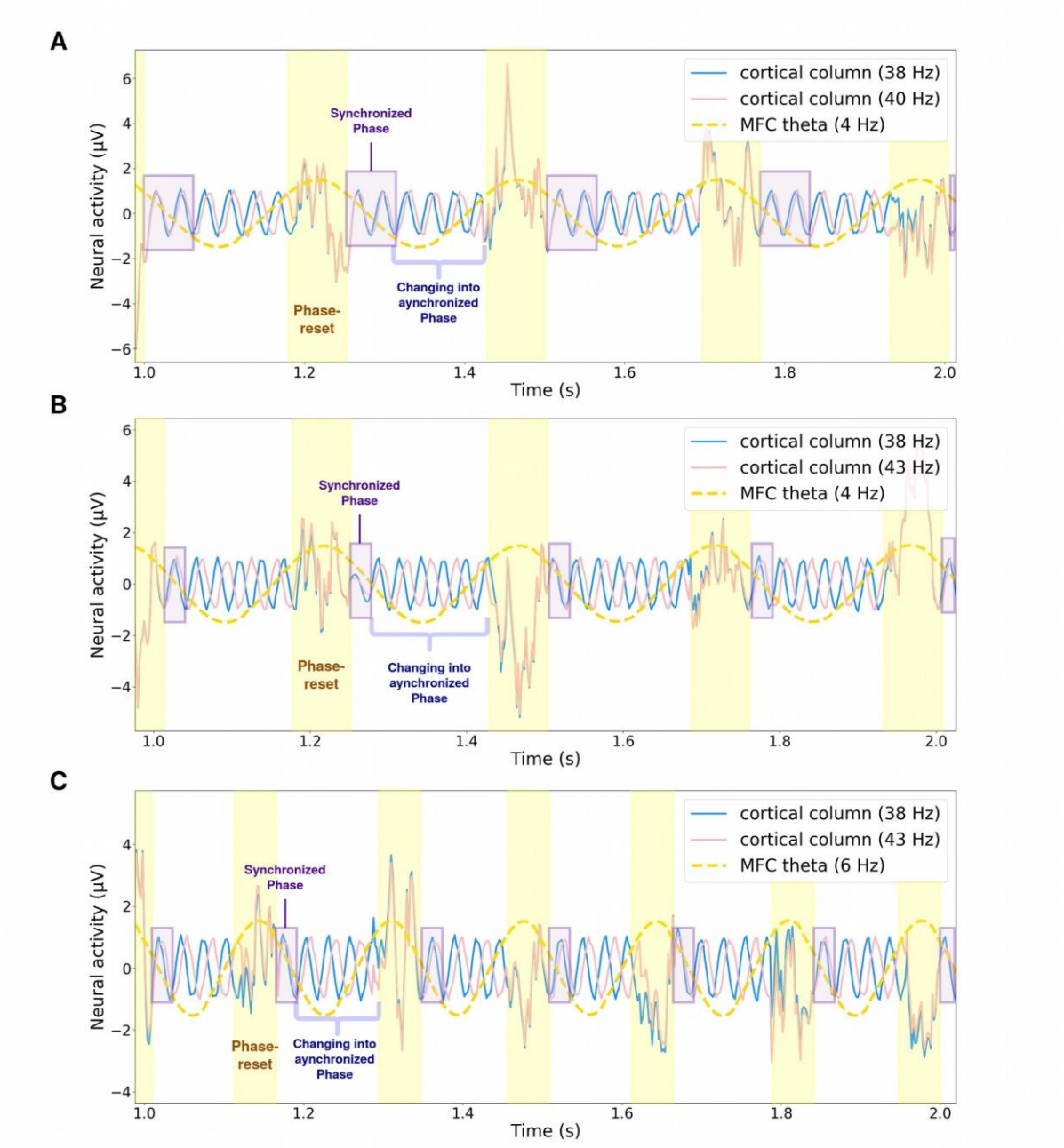

Figure 13. A demonstration of the sync-model performing on a stimulus-response mapping task trial with varying MFC theta and gamma variability. **A.** *The MFC is set to 4 Hz and the gamma variability to 2 Hz. The sensory unit (i.e. cortical column) has a gamma frequency of 38 Hz and the response unit has a gamma frequency of 40 Hz* **B.** *The MFC is set to 4 Hz and the gamma variability to 5 Hz. The sensory unit has a gamma frequency of 38 Hz and the response unit has a gamma frequency of 43 Hz* **C.** *The MFC is set to 6 Hz and the gamma variability to 5 Hz. The sensory unit has a gamma frequency of 38 Hz and the response unit has a gamma frequency of 43 Hz.*

variables.

RT distributions are affected by gamma variability (Figure 15). With larger gamma variability, RT distributions became bimodal. This is an interesting observation

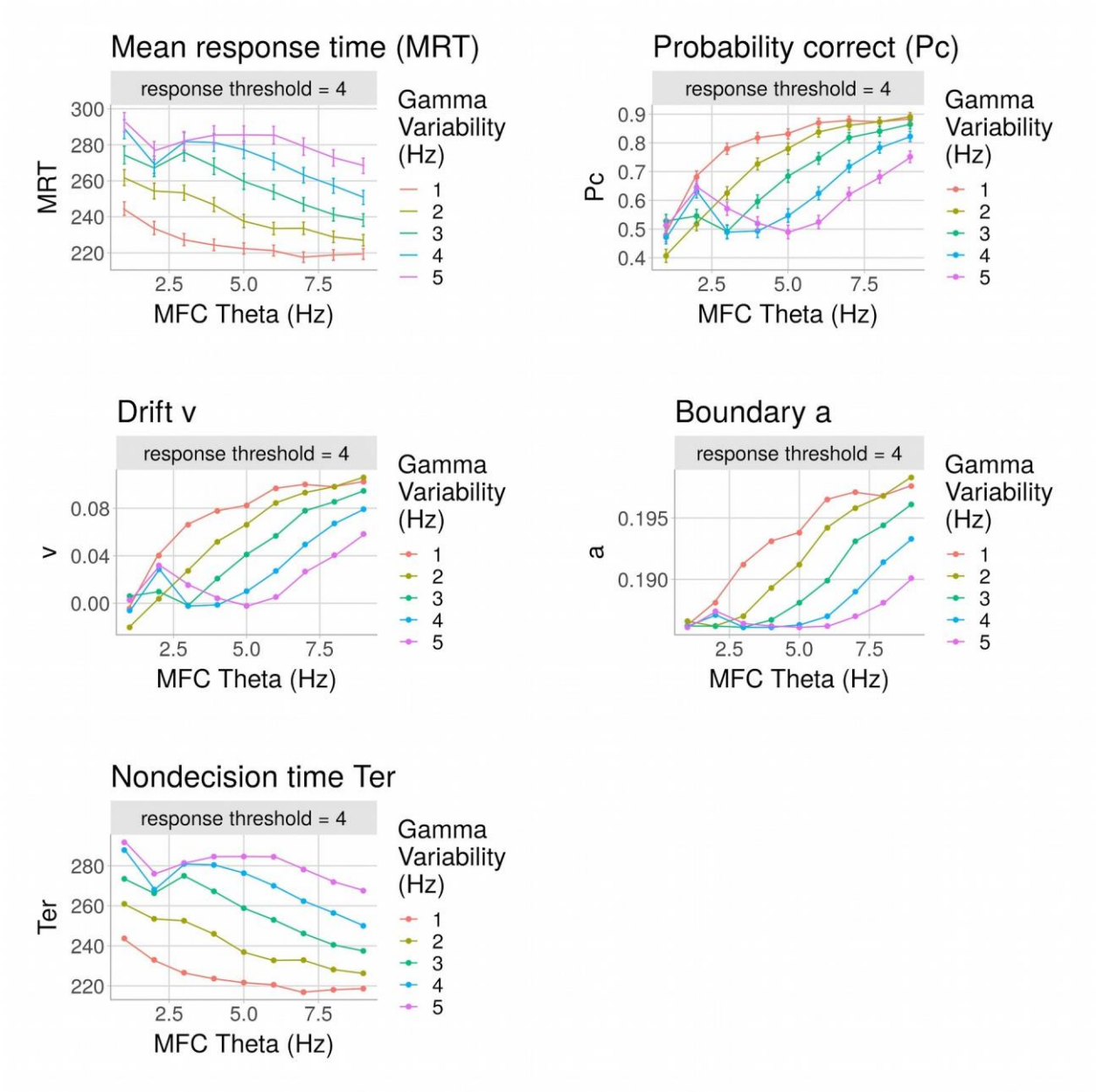

Figure 14. Multiple plots showing the performance variables across MFC theta and gamma variability values. *Across all performance variables, a higher MFC theta and a lower gamma variability both result in the best model behavioral performance.*

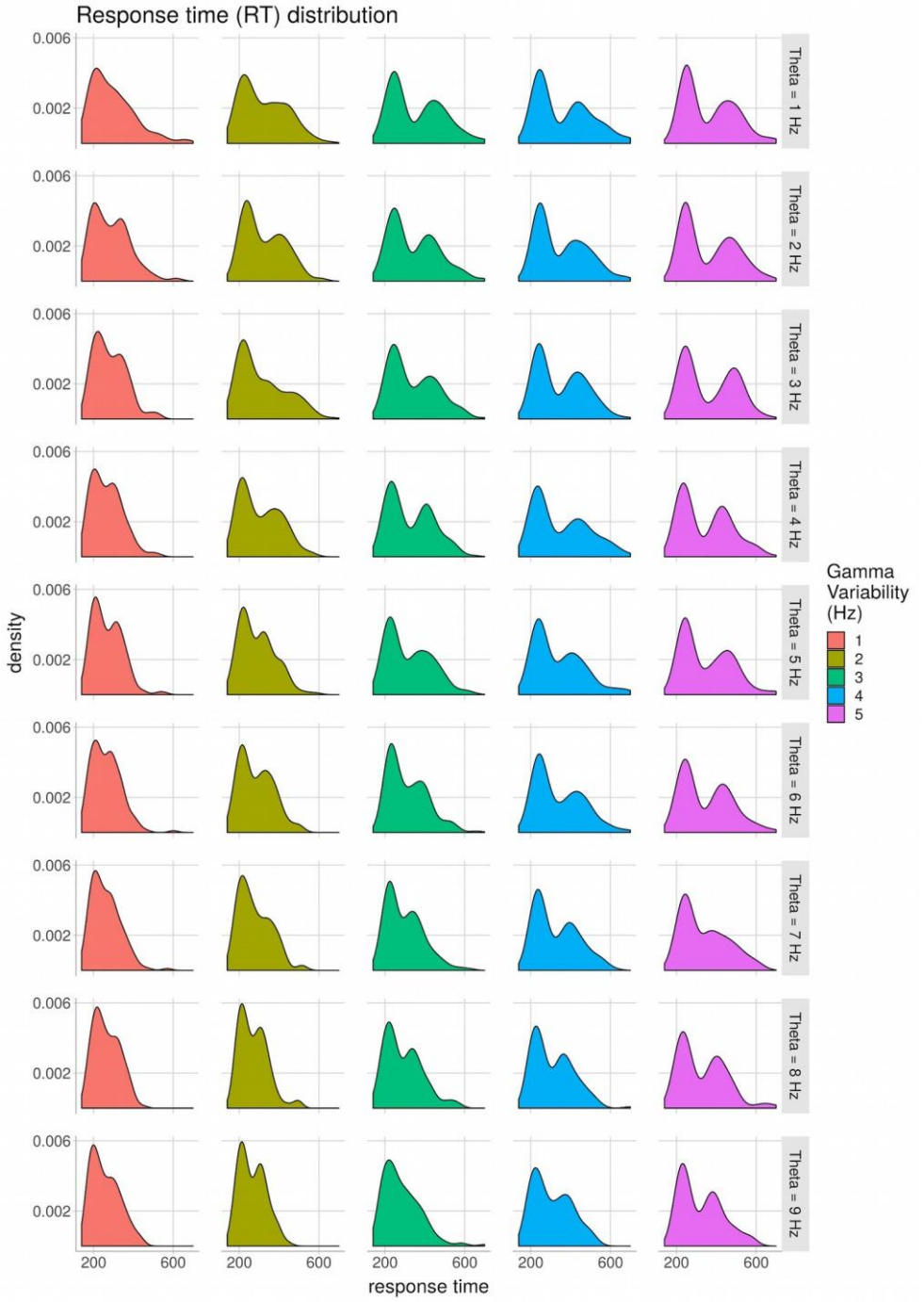

Figure 15. RT distributions across MFC theta and gamma variability values. *With larger gamma variability, RT distributions become bimodal. With increasing MFC theta, RT distributions become narrower.*

because empirical RT distributions are typically unimodal. Furthermore, in the empirical RT distributions of Senoussi et al. (2018) (Figure 16), some participants do show a bi-

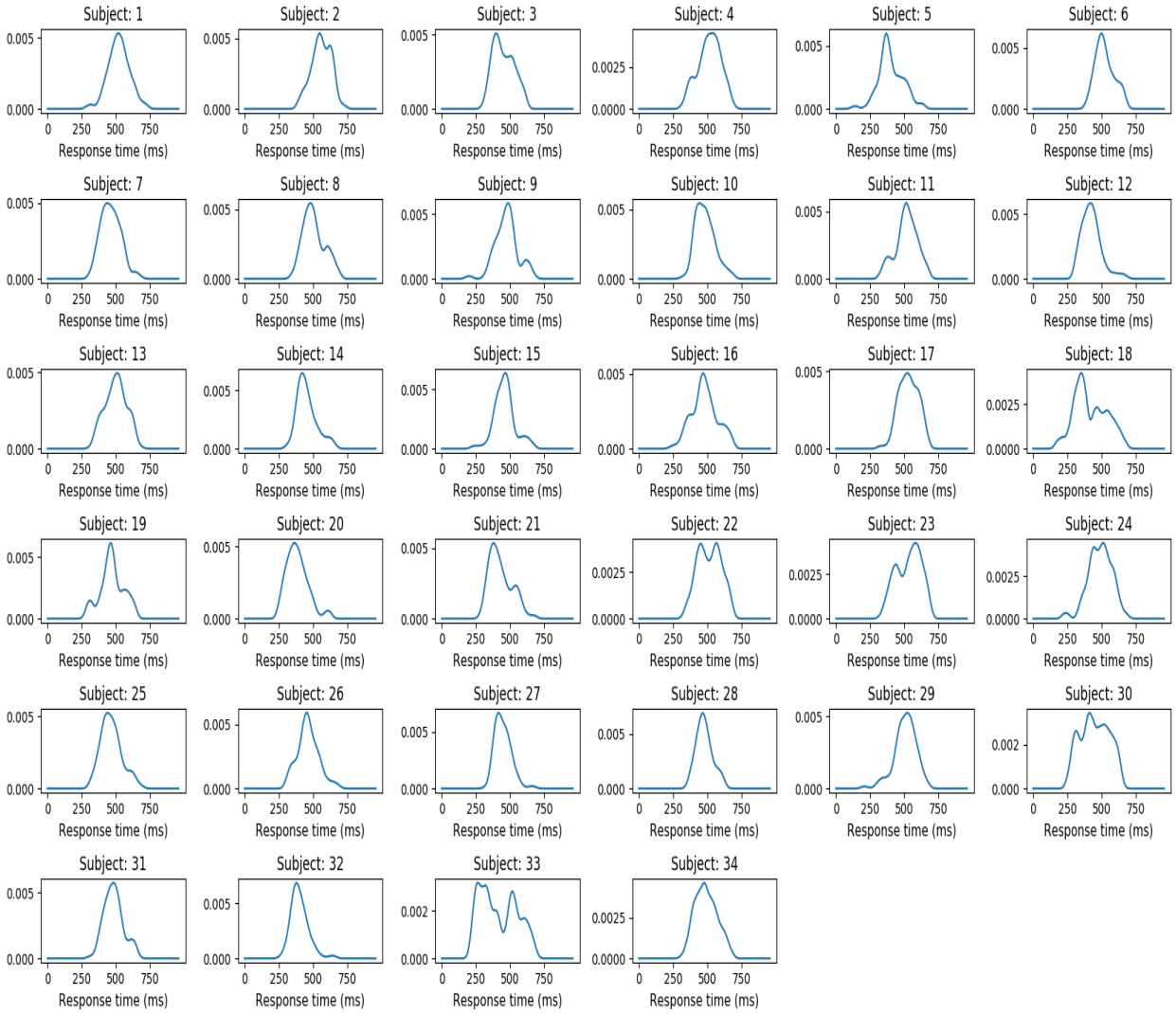

Figure 16. Empirical RT distributions from Senoussi et al. (2018). *Some participants show an unimodal RT distribution, while others show a bi-modal RT distribution.*

modal distribution.

MFC theta. The MFC theta parameter varied between 1 Hz to 9 Hz. The focus was put on the theta-band oscillations, but a few delta-band frequencies (1-3 Hz) and alpha-band frequencies (8-9 Hz) were included because setting the theta-band limits between 4 and 7 Hz is an arbitrary limit that has been shown to vary across individuals (Klimesch, 1999). Therefore, we included neighboring frequencies to have a broader view of theta oscillations. The number of noise bursts being sent each second to task-relevant

cortical columns are equal to the MFC theta value, demonstrated in figure 13B-C. Thus, a high MFC theta value leads to more frequent phase-synchronization events between task-relevant units. This affected behavioral performance (Figure 14). Higher MFC theta values resulted in better task performance across all performance measures.

An interesting observation in the performance measures can be seen in Figure 14 and are highlighted in Figure 17. When the MFC theta value gets closer to being equal to the gamma variability value the performance is worse. This is most visible when the gamma variability is higher than 2. This might be attributed to an artefact of the sync-model's implementation being too "precise". Indeed, when the gamma variability was higher than 2 and a multiple of the MFC theta frequency, phase-synchronizing bursts did not synchronize task-relevant processing units because they reached processing units precisely when the two units were back in synchrony. In the quantitative analysis, we decided to avoid these artifacts by not using gamma variability values above 2.

Lower MFC theta values flattened the RT distribution more (Figure 15), while higher MFC theta values made the RT distributions narrower.

Response threshold. The response threshold parameter varied between 1 and 5 but only values between 3 and 5 were included in the parameter space exploration. Response threshold values below 3 led to RT distributions that are too different from empirical RT distributions.

At MFC theta values above 5 Hz the speed-accuracy trade-off is visible for all the response threshold values; Among response threshold values a higher response threshold sacrifices speed for more accuracy (Figure 18); this is reflected in a higher number of correct trials (Pc) but also in an increase in MRT.

Higher response threshold values led to flatter RT distributions and, as can be expected, led to longer RT (Figure 19). This is an interesting behavioral variability that might help us in recovering which response threshold value is associated with which RT distribution.

Quantitative analysis: parameter recovery analysis

To conduct the parameter recovery analysis, we developed a fitting function. This consisted of an error function and that was used in a fitting algorithm. For the fitting

algorithm, we used differential evolution (Storn & Price, 1997). The error function used performance measures (i.e. response time and accuracy) to provide an error measure to the fitting algorithm to distinguish between different values of a sync-model parameter.

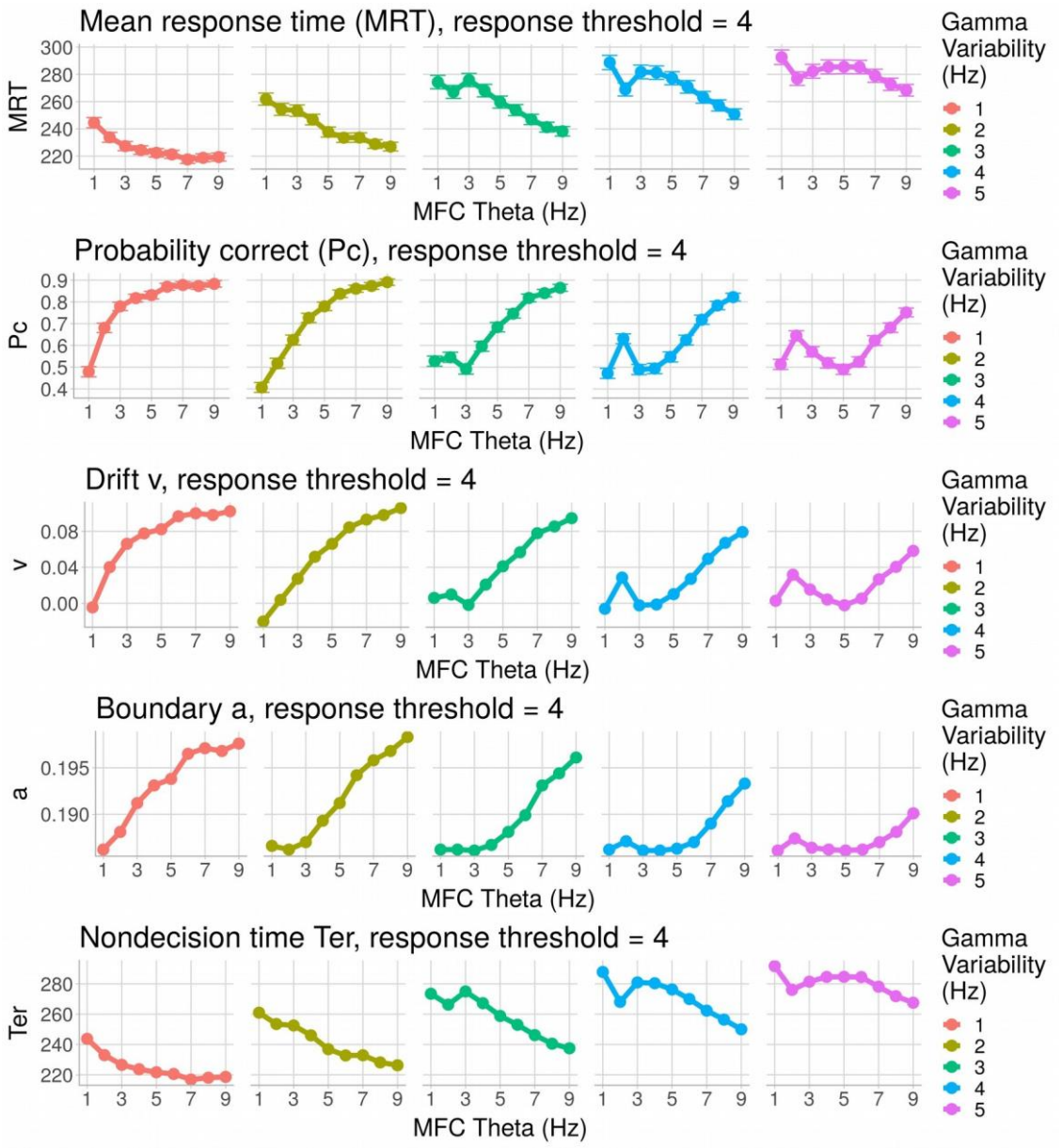

Figure 17. Artifacts in sync-model behavioral performance. *Across all performance variables, when the MFC theta value gets closer to being equal to the gamma variability value the performance is worse. This is most visible when the gamma variability is higher than 2.*

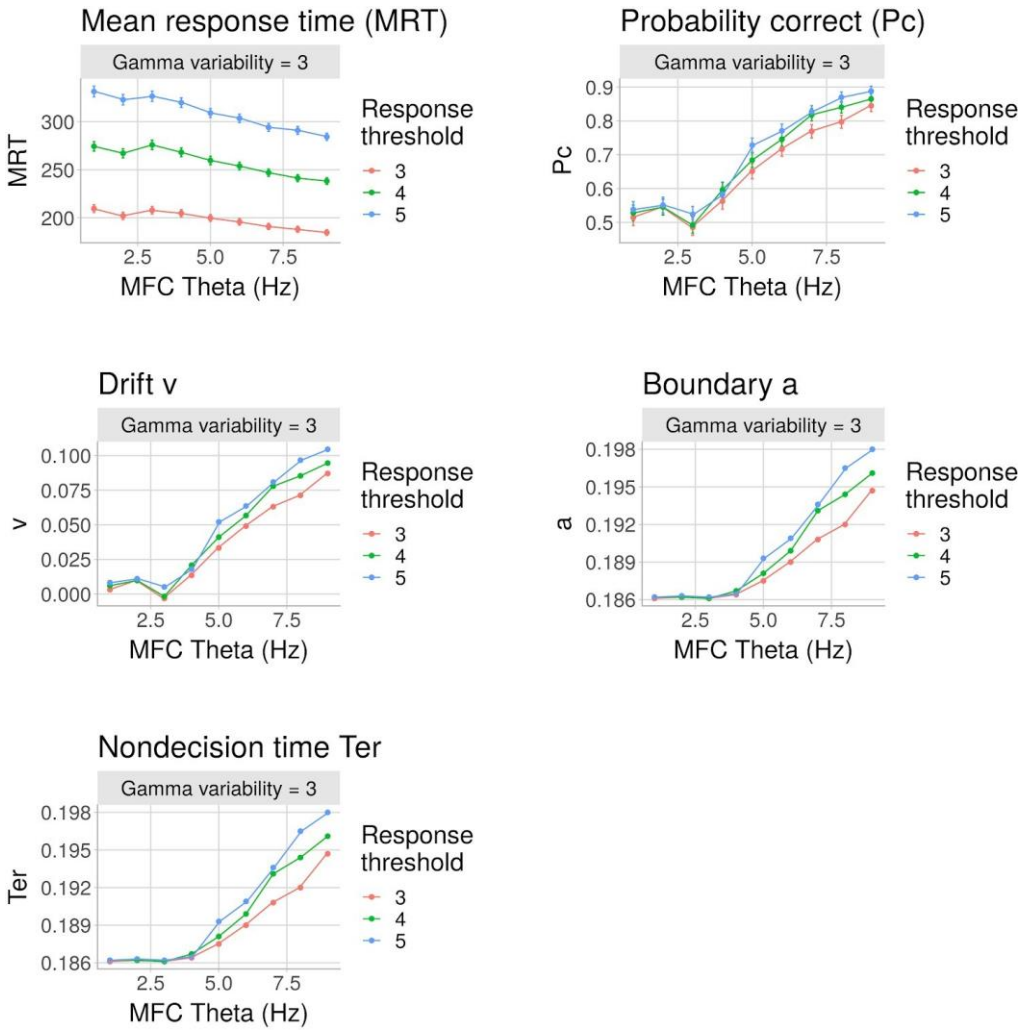

Figure 18. *S*peed-accuracy trade-off in response threshold values. *At MFC theta values above 5 Hz, the speed-accuracy trade-off is visible on the performance variables. High values of response threshold lead to a higher Pc, a larger v, and a larger a but a slower MRT and larger non-decision time.*

Next, sync-model behavior was generated with a set of known parameter values (i.e., target data). Then, the fitting function attempted to recover one or more of these parameter values by using the sync-model to generate new behavioral data (i.e., simulated data) and comparing these to the target data.

Response threshold recovery. The parameter space exploration showed that

the mass of the RT distribution (Figure 19) shifts on the x-axis across different response threshold measures. A standard error function that compares RT distributions was used; it is illustrated in Figure 20. This error function calculates how much two RT distributions differ from each other. More specifically, the correct RT distribution (i.e., response times of correct trials) of the simulated data were subtracted from the correct RT distributions of the target data. The same was done for the error RT distributions (i.e., response times of incorrect trials).

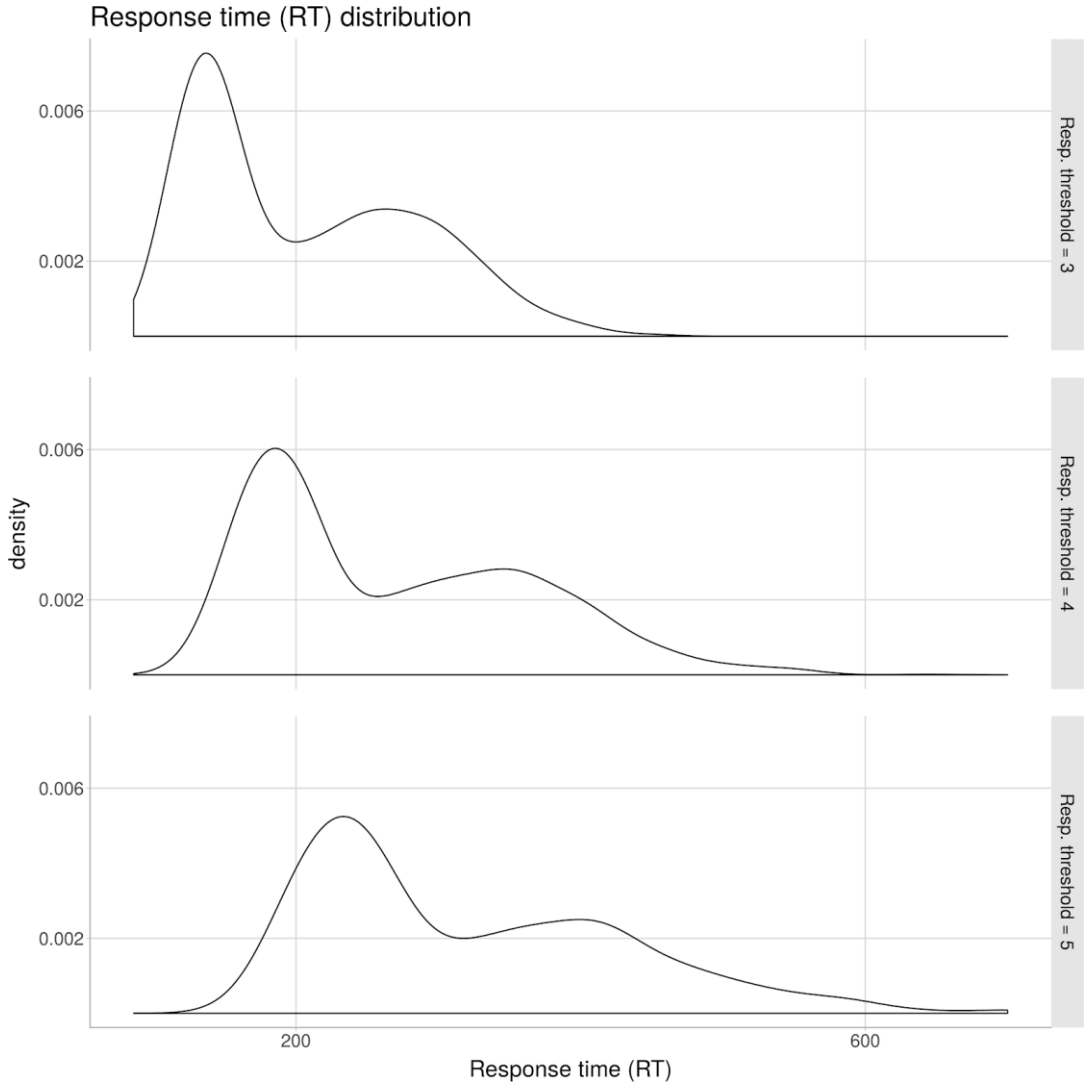

Figure 19. RT distributions across response threshold values. *A response threshold of 5 flattens the RT distribution more and has slower RTs than lower response threshold values.*

In this first parameter recovery, we were only interested in investigating if the response value was identifiable based on the RT distributions. To reduce complexity, the fitting function was given the correct MFC theta and gamma variability values of the target data (i.e., the MFC theta and gamma variability were fixed). The goal of the fitting function was to only recover the response threshold value. The fitting function was perfectly able to recover the response threshold using a standard error function based on RT distributions (Figure 21).

MFC theta recovery. The same approach was used to recover the MFC theta value. The response threshold and the gamma variability were fixed, and the fitting function was given the same error function (Figure 20). This failed to recover the MFC theta values, as shown in Figure 22.

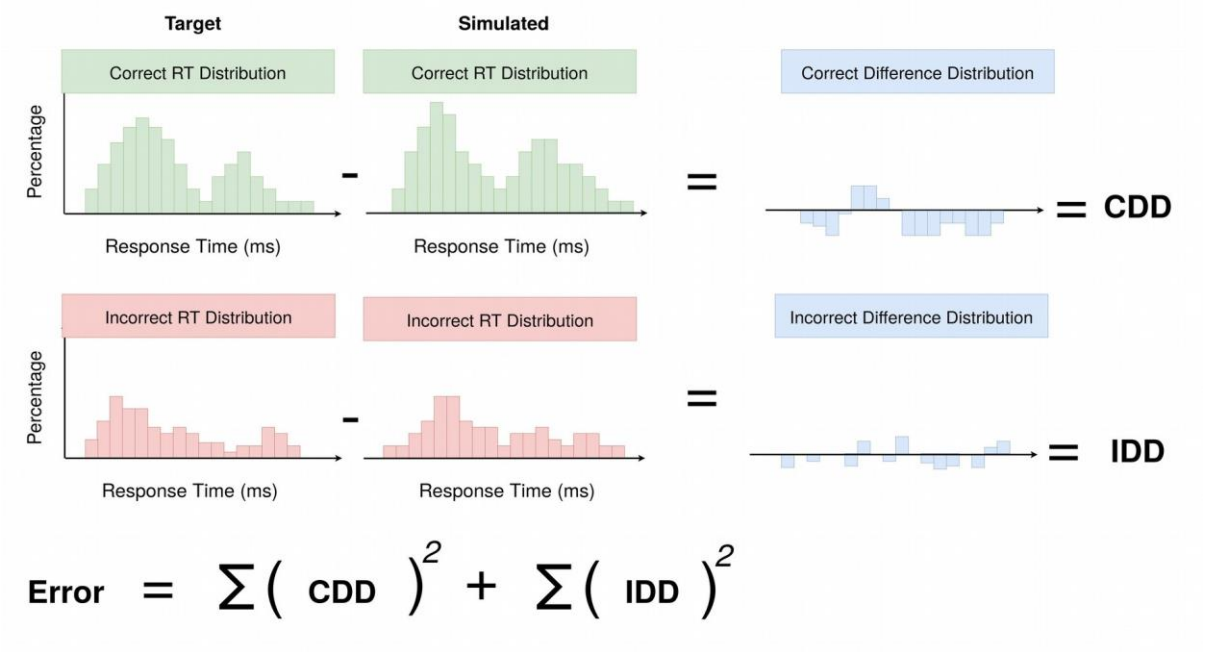

Figure 20. An illustration of a standard error function based on RT distributions. *First, the correct RT distribution (i.e., response times of correct trials) of the simulated data is subtracted from the correct RT distribution of the target data, resulting in a correct RT difference distribution. The same is done for the incorrect RT distributions (i.e., response times of incorrect trials), leading to an incorrect RT difference distribution. In the next step, the summation of the correct RT difference distribution is taken and then squared (i.e., correct RT error). The same is done for the incorrect RT difference distribution. In the last step, the correct RT error is added together with the incorrect RT error.*

This compelled us to try to develop a new error function that captures behavioral characteristics that vary across MFC theta values. The model simulations from the parameter space exploration were re-analyzed and we identified discriminative characteristics of RT distributions (Figure 23). Based on this, a customized term for the error function, based on the relative height of the first peak of RT distributions, was

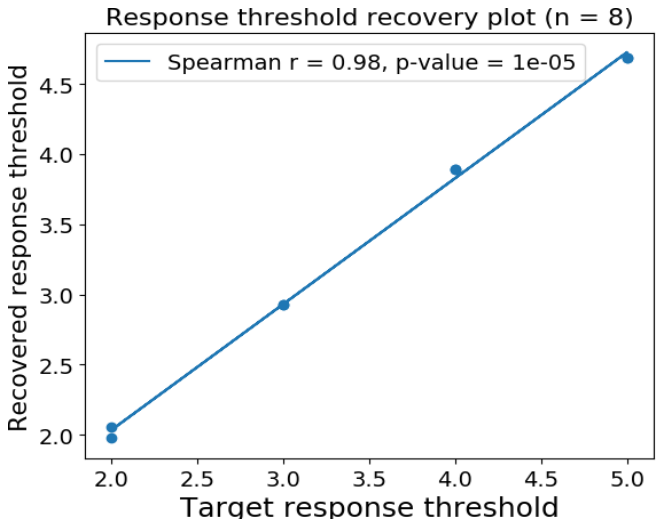

Figure 21. Response threshold recovery plot. All the target response threshold values ($n\ simulations = 8$) were successfully recovered (r=0.98).

developed, see Figure 24.

Using this error function, the MFC theta values were perfectly recoverable, as shown in Figure 25.

MFC theta and response threshold recovery. In this next recovery, only the gamma variability was fixed. Both previously described error functions (Figure 20 and 24) were used to form a combined error function, see Equation 1. this error function allowed to recover the MFC theta and the response threshold at the same time, as shown in Figure 26.

$$Error = \sum (CDD)^2 + \sum (IDD)^2 + (TRPH - SRPH)^4 \quad (1)$$

Gamma variability recovery. As discussed in the parameter recovery analysis,

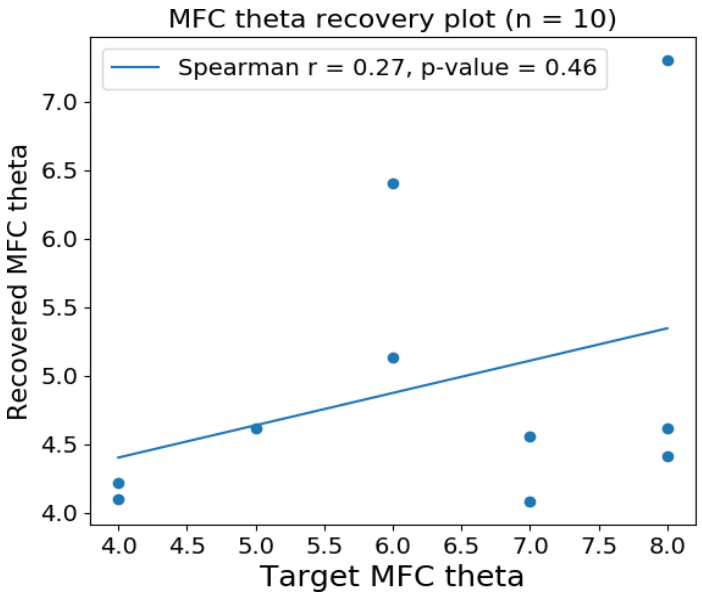

Figure 22. Failed MFC theta recovery plot. *Most of the target MFC theta values (n simulations = 10) were not recoverable.*

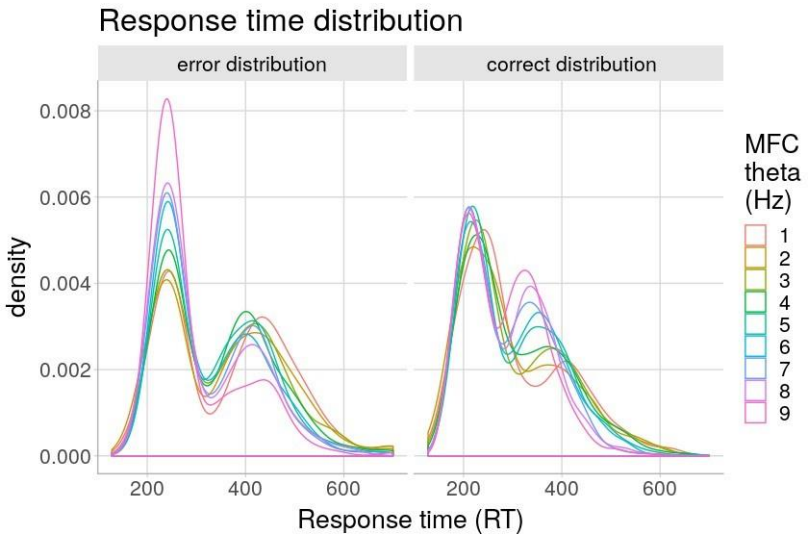

Figure 23. MFC theta discriminative characteristics of RT distributions. *The error (i.e., incorrect) RT distributions can discriminate between different MFC theta values through the height of the first peak. In correct bi-modal RT distributions, the second peak is also discriminative.*

Figure 24. An illustration of a customized error function based on RT peaks. *In the target data, the first peak from the correct and incorrect RT distributions is selected. The target data's relative peak height (TRPH) is calculated by dividing the highest correct RT peak by the highest incorrect RT peak. In the same way, the relative peak height is calculated for the simulated data (SRPH). To calculate the total error, the SRPH is subtracted from the TRPH, then, the error is scaled by taking it to the power of 4. This scaling makes sure that the error of this error function is around the same size as the error from the error function in Figure 20.*

the gamma variability contained artefacts. For this reason, we developed no error function the gamma variability.

Quantitative analysis: participant fitting

The parameter recovery analysis was a success, showing that the error functions work. Although we did not develop an error function for the gamma variability, we still

proceeded with applying the fitting function to empirical data from Senoussi et al. (2018). Twenty-three participants were selected based on the number of trials that they had

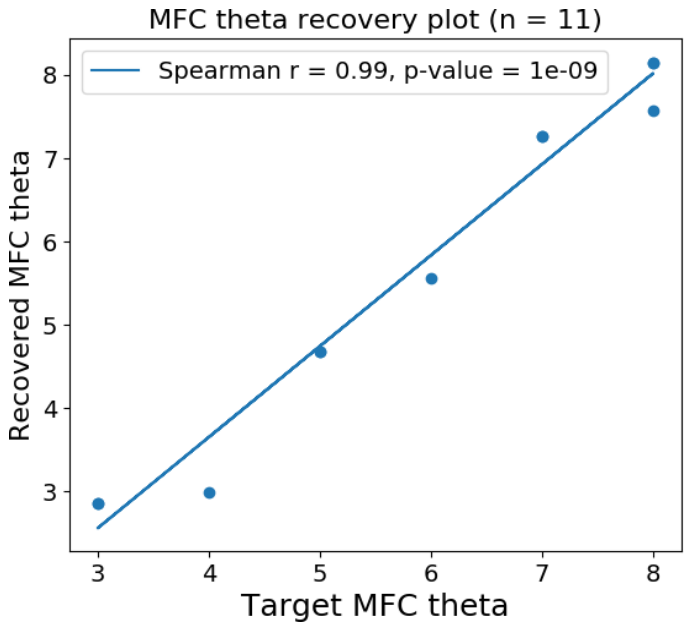

Figure 26. MFC theta recovery plot. *The target MFC theta values (n = 11) were successfully recoverable (r = 0.99)*

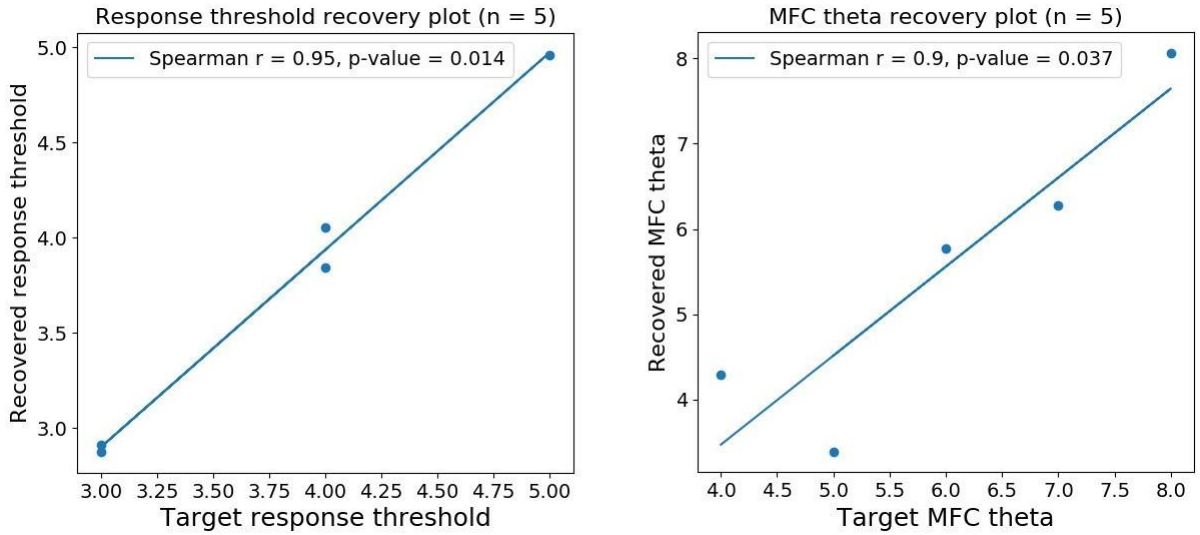

Figure 25. MFC theta and response threshold recovery plot. *The target MFC theta values (n = 5) and the target response threshold values (n = 5) were successfully recoverable together.*

completed. For all participants, the gamma variability was fixed at 2 (to avoid artifacts) and ran the fitting function to fit the MFC theta and response threshold. We then proceeded to correlate the fitted MFC theta with the performance measures, see Figure 27.

Participants' fitted MFC theta has a significant negative relationship (r=−0.51, p=0.01) with participants' MRT. Thus, consistent with what the parameter exploration analysis showed, a higher MFC is associated with a faster MRT. Although other performance measures didn't show a significant relationship with the fitted MFC theta, the trend shown is consistent with the model behavioral patterns in the parameter exploration analysis.

The peak frequency of each subject was correlated with their fitted MFC theta (Figure 27F). There is a small positive trend, but no significant relationship.

Discussion

A computational approach was taken in studying the relationship between theta-band oscillations and cognitive control. We tried to answer the following two questions:
(1) How does theta oscillation frequencies affect performance in a cognitive control task?
(2) Can theta oscillation frequencies explain inter-individual variability in cognitive control? First, we will discuss these questions based on the results of the qualitative. Second, we will discuss these questions based on the quantitative analysis

Qualitative analysis: parameter exploration analysis

(1) MFC theta. The qualitative analysis taught us that individual MFC theta frequencies lead to better overall performance on cognitive control.

The parameter exploration shows us that higher MFC theta frequencies lead to a higher number of temporal windows in which task-relevant units are phase-synchronized, leading to efficient task performance (Figure 13B-C). These temporal windows provide effective communication between rate code neurons in task-relevant units of the model.

The parameter exploration also reveals that although the sync-model is built up around theta-band oscillations, alpha-band oscillation frequencies (8 Hz and 9 Hz in our study) lead to better performance on the cognitive control task. This does not fit with empirical evidence (Cavanagh & Frank, 2014; Gratton et al., 2018), which suggests that

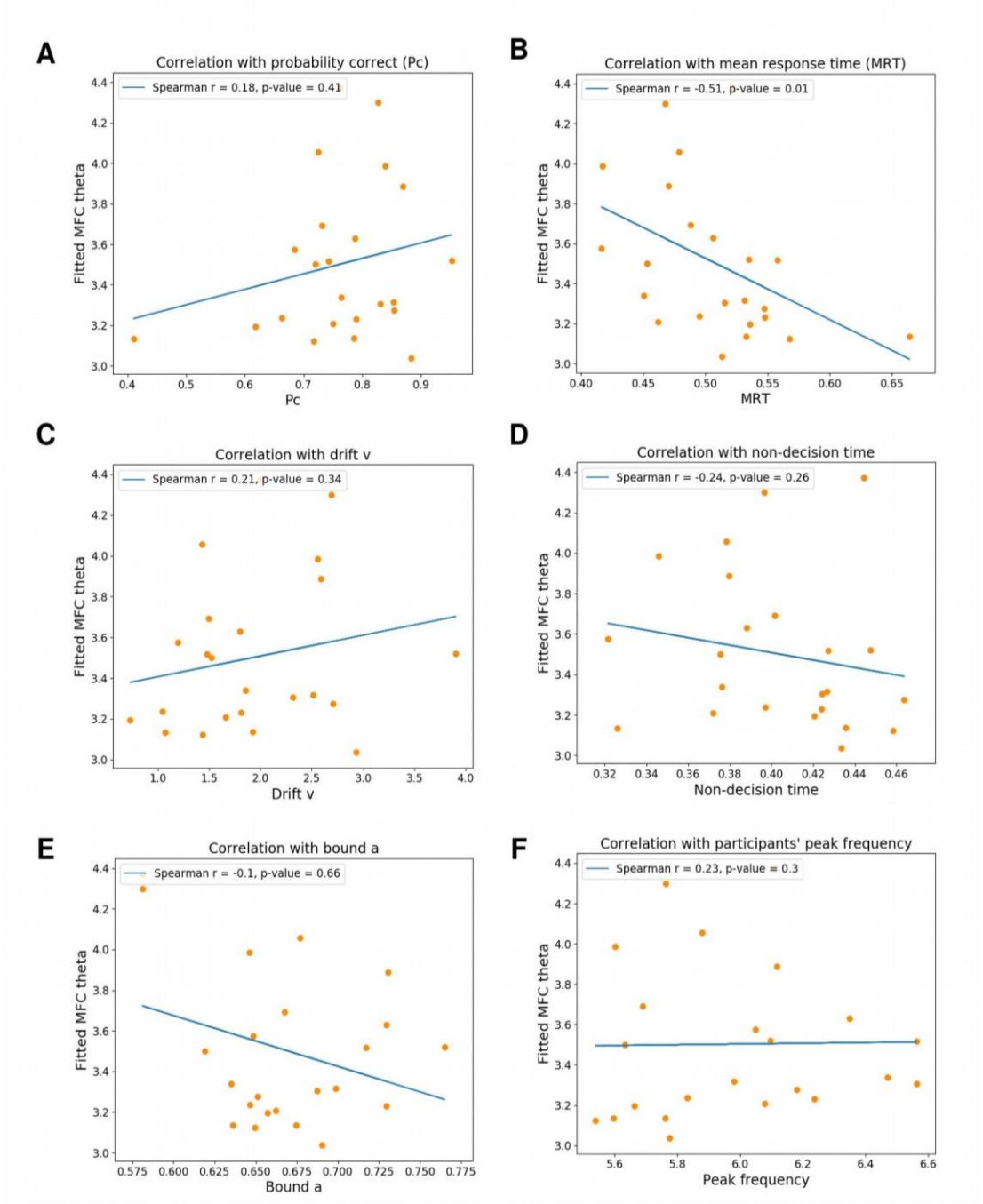

Figure 27. Correlation between fitted MFC and behavioral EEG variables. *All the participants' performance variables showed a relationship trend consistent with the model behavioral performance in the parameter exploration analysis but only the correlation with the MRT (***B***) is significant (*r*=−0.51, *p*=0.01). **F.** The participants' EEG peak frequency on the task shows a small positive relationship with the fitted MFC theta.*

additional biological constraints might need to be incorporated to better understand the interplay between frequency bands in different cognitive processes. Alpha-band oscillations have been shown to sub serve processes in reactive control (i.e., inhibition) (Pani et al., 2014).

Both gamma variability and the response threshold affected the sync-model's behavioral performance on the task in interaction with MFC theta.

Gamma variability. The higher the gamma variability, the worse the overall sync-model performance. This behavioral pattern is consistent with the CTC theory: the larger the difference between gamma oscillations' frequencies, the more difficult it is to synchronize them, and thus. the worse the communication between them, which should lead to worse performance. This is also coherent with previous work, for instance, a study by Siegle et al. (2014) found that gamma-range synchronization enhanced the detection of tactile stimuli.

Furthermore, the gamma frequencies were kept on average around 40 Hz for each unit in the sync-model and we focused the manipulations on the gamma variability. We do not know how behavioral performance will be affected when the gamma frequencies are also manipulated between 25 to 150 Hz (the typical range of frequencies attributed to the gamma-band).

Response threshold. The response threshold could be used to affect the speed-accuracy trade-off, but only when the MFC theta frequency was higher than 5 Hz. A higher response threshold required to accumulate more information before deciding on what response to give in a trial. This is reflected in a higher accuracy but a slower RT.

(2) Inter-individual variability. If we consider each sync-model simulation as an individual entity, then yes, the MFC theta, gamma variability, and response threshold lead clearly to inter-individual variability in performance.

Unexpected results. We found that when the gamma variability value is closer to being a multiple of the MFC theta value the performance drops, we call these performance throughs (Figure 17). These performance throughs were most visible when the gamma variability was higher than 2.

This happened because of the periodic nature of these signals. When processing units (stimulus and response) are different (i.e. when gamma variability is not zero), their

phase-synchrony shifts with time after a burst. One oscillation goes “faster” than the other, so its peak gets further and further from the other oscillation. But because of the cyclic nature of this process, the phase of the faster oscillation eventually reaches the peak of the “next” peak of the slower oscillation. In other words, after a burst, the peak of the faster oscillation happens at the same time as the peak of the slower oscillation, but with time it gradually shifts to later phases of the slower oscillations. At some point, the peak of the faster oscillation reaches another peak of the slower oscillation, which makes them synchronized again. This is not an issue in general, but when the gamma variability, which determines how fast the two gamma frequencies shift relative to each other, is a multiple of the MFC theta frequency value, the burst is sent exactly when the two oscillations are back in synchrony. Therefore, the burst has no supplementary effect on the synchrony of these oscillations and makes the mechanism implements through theta oscillations completely ineffective. This artifact of the model implementation incidentally demonstrates that bursts sent by the MFC do have a positive influence on the model performance as when they are not effective (in the case of gamma variability being a multiple of the MFC theta frequency presented here), model performance drops.

Quantitative analysis: parameter recovery analysis

MFC theta and response threshold. We were able to successfully recover MFC theta and response threshold values by developing error functions that solely relied on RT distributions. Different characteristics of the RT distributions vary across parameters’ values. The mass of the RT distributions (Figure 19) shifts on the x-axis across response threshold values. The RT distribution peak of the incorrect trials varies across MFC theta values (Figure 24). Thus, the RT distributions are very informative about unobserved neural and psychological mechanisms. This is a great advantage. Every cognitive task can easily measure the RT on each trial. This suggests that it is possible to fit the sync-model on any cognitive task and use it further built our understanding of cognitive control.

Gamma variability. We did not develop an error function to recover the correct gamma variability because the performance throughs artefacts.

The behavioral patterns of the gamma variability are also intertwined with the

behavioral patterns of the MFC theta. Thus, making it more difficult to recover both MFC theta values and gamma variability values at the same time. One possible behavioral pattern that might help us in dissociating MFC theta values from gamma variability values is the RT distribution space, specifically if the shape is unimodal or bimodal (Figure 14). But not every cognitive task might lead to the observation of bi-modal shaped RT distributions.

Quantitative analysis: participant fitting

(1) MFC theta. We were not able to generalize most of the results from the qualitative analysis to the quantitative analysis. Although all performance measures did show a trend similar to the patterns found in the qualitative analysis, only the MRT showed a significant correlation with the fitted MFC values (r=−0.51, p=0.01), see Figure 27.

(2) inter-individual variability. Figure 27 still shows a lot of unexplained inter-individual variability on all the performance measures. Although the fitted MFC values can explain a portion of MRT inter-individual variability, the evidence is still lacking for the other performance measures.

Limitations. The following reasons might explain as to why the participant fitting was not able show a stronger trend across the performance variables:

First, while in the sync-model's behavioral performance we were able to dissociate MFC theta values from gamma variability values (e.g. comparing MFC values while the gamma variability is fixed), we weren't able to achieve this amount of parameter control in the participant fitting. Hypothetically, if all the participants fitting resulted in the same gamma variability value, then the relationship between MFC theta and behavioral performance could be more easily compared to the behavioral pattern seen in the sync-model.

Second, in this study we compared the performance of the participants' fitted MFC theta values to the performance of the sync-model's MFC theta values. This might not be the best way to approach it. Another way would be to compare behavioral patterns based on parameter pairs. This means that MFC theta values and gamma variability values are combined into one measure. For example, participant "A" has a

fitted MFC theta of 5 Hz and participant “B” has a fitted MFC theta of 6 Hz. Based on the qualitative analysis, we suspect that participant “B” has performed better on the task. But we notice that participant “A” actually has a better task performance than participant “B”. Now, we bring in their fitted gamma variability values. Participant “A” has a fitted gamma variability of 3, while participant “B” has a fitted gamma variability of 4. Figure 14 tells us indeed participant “A” (with an MFC theta of 5 Hz, and a gamma variability of 3) performs better than participant “B” (with a MFC theta of 6 Hz, and a gamma variability of 4). This is the reason why it might be more interesting if we could compare parameter pairs instead of comparing single parameters. Using this approach, it might be possible to explain a bigger portion of inter-individual variability on task performance.

Implications and conclusion.

The sync-model has shown to be a great asset in the study of cognitive control (Verbeke et al., 2020; Verbeke & Verguts, 2019). Not only does the sync-model allow to model and analyze how neural and psychological mechanisms result in cognitive control, but it could also permit us to analyze empirical data and fit the sync-model to it. Further improvements to the model such as fixing the performance throughs and developing an error function for the gamma variability can lead to a powerful improvement of this computational model that would increase its use as a tool to study cognitive control and allow us to extract neural and psychological mechanisms on any cognitive control task.

Bibliography

Adam, N., Blaye, A., Gulbinaite, R., Delorme, A., & Farrer, C. (2020). The role of midfrontal theta oscillations across the development of cognitive control in preschoolers and school-age children. *Developmental Science*. https://doi.org/10.1111/desc.12936

Axmacher, N., Henseler, M. M., Jensen, O., Weinreich, I., Elger, C. E., & Fell, J. (2010). Cross-frequency coupling supports multi-item working memory in the human hippocampus. *Proceedings of the National Academy of Sciences*, *107*(7), 3228–3233. https://doi.org/10.1073/pnas.0911531107

Bonnefond, M., Kastner, S., & Jensen, O. (2017). Communication between Brain Areas Based on Nested Oscillations. *Eneuro*, *4*(2), ENEURO.0153-16.2017. https://doi.org/10.1523/ENEURO.0153-16.2017

Breukelaar, I. A., Antees, C., Grieve, S. M., Foster, S. L., Gomes, L., Williams, L. M., & Korgaonkar, M. S. (2017). Cognitive control network anatomy correlates with neurocognitive behavior: A longitudinal study: Cognitive Control Network Development. *Human Brain Mapping*, *38*(2), 631–643. https://doi.org/10.1002/hbm.23401

Canolty, R. T., Edwards, E., Dalal, S. S., Soltani, M., Nagarajan, S. S., Kirsch, H. E., Berger, M. S., Barbaro, N. M., & Knight, R. T. (2006). High Gamma Power Is Phase-Locked to Theta Oscillations in Human Neocortex. *Science*, *313*(5793), 1626–1628. https://doi.org/10.1126/science.1128115

Cavanagh, J. F., & Frank, M. J. (2014). Frontal theta as a mechanism for cognitive control. *Trends in Cognitive Sciences*, *18*(8), 414–421. https://doi.org/10.1016/j.tics.2014.04.012

Colgin, L. L. (2016). Rhythms of the hippocampal network. *Nature Reviews Neuroscience*, *17*(4), 239–249. https://doi.org/10.1038/nrn.2016.21

Douglas, R. J., Martin, K. A. C., & Whitteridge, D. (1989). A Canonical Microcircuit for Neocortex. *Neural Computation*, *1*(4), 480–488. https://doi.org/10.1162/neco.1989.1.4.480

Eigsti, I.-M., Zayas, V., Mischel, W., Shoda, Y., Ayduk, O., Dadlani, M. B., Davidson, M. C., Aber, J. L., & Casey, B. J. (2006). Predicting Cognitive Control From Preschool to Late Adolescence and Young Adulthood. *Psychological Science*, *17*(6), 478–484. https://doi.org/10.1111/j.1467-9280.2006.01732.x

Friedman-Hill, S. (2000). Dynamics of Striate Cortical Activity in the Alert Macaque: I. Incidence and Stimulus-dependence of Gamma-band Neuronal Oscillations. *Cerebral Cortex*, *10*(11), 1105–1116. https://doi.org/10.1093/cercor/10.11.1105

Fries, P., Roelfsema, P. R., Engel, A. K., Konig, P., & Singer, W. (1997). Synchronization of oscillatory responses in visual cortex correlates with perception in interocular rivalry.

Proceedings of the National Academy of Sciences, *94*(23), 12699–12704. https://doi.org/10.1073/pnas.94.23.12699

Fries, Pascal. (2005). A mechanism for cognitive dynamics: neuronal communication through neuronal coherence. *Trends in Cognitive Sciences*, *9*(10), 474–480. https://doi.org/10.1016/j.tics.2005.08.011

Fries, Pascal. (2015). Rhythms for Cognition: Communication through Coherence. *Neuron*, *88*(1), 220–235. https://doi.org/10.1016/j.neuron.2015.09.034

Fries, Pascal, Schröder, J.-H., Roelfsema, P. R., Singer, W., & Engel, A. K. (2002). Oscillatory Neuronal Synchronization in Primary Visual Cortex as a Correlate of Stimulus Selection. *The Journal of Neuroscience*, *22*(9), 3739–3754. https://doi.org/10.1523/JNEUROSCI.22-09-03739.2002

Gillie, B. L., & Thayer, J. F. (2014). Individual differences in resting heart rate variability and cognitive control in posttraumatic stress disorder. *Frontiers in Psychology*, *5*. https://doi.org/10.3389/fpsyg.2014.00758

Gratton, G., Cooper, P., Fabiani, M., Carter, C. S., & Karayanidis, F. (2018). Dynamics of cognitive control: Theoretical bases, paradigms, and a view for the future. *Psychophysiology*, *55*(3), e13016. https://doi.org/10.1111/psyp.13016

Gray, C. M., König, P., Engel, A. K., & Singer, W. (1989). Oscillatory responses in cat visual cortex exhibit inter-columnar synchronization which reflects global stimulus properties. *Nature*, *338*(6213), 334–337. https://doi.org/10.1038/338334a0

Holmes, A. J., Hollinshead, M. O., Roffman, J. L., Smoller, J. W., & Buckner, R. L. (2016). Individual Differences in Cognitive Control Circuit Anatomy Link Sensation Seeking, Impulsivity, and Substance Use. *The Journal of Neuroscience*, *36*(14), 4038–4049. https://doi.org/10.1523/JNEUROSCI.3206-15.2016

Karayanidis, F., Whitson, L. R., Heathcote, A., & Michie, P. T. (2011). Variability in Proactive and Reactive Cognitive Control Processes Across the Adult Lifespan. *Frontiers in Psychology*, *2*. https://doi.org/10.3389/fpsyg.2011.00318

Klimesch, W. (1999). EEG alpha and theta oscillations reflect cognitive and memory performance: a review and analysis. *Brain Research Reviews*, *29*(2–3), 169–195. https://doi.org/10.1016/S0165-0173(98)00056-3

Kriegeskorte, N., & Douglas, P. K. (2018). Cognitive computational neuroscience. *Nature Neuroscience*, *21*(9), 1148–1160. https://doi.org/10.1038/s41593-018-0210-5

Landau, A. N., Schreyer, H. M., van Pelt, S., & Fries, P. (2015). Distributed Attention Is Implemented through Theta-Rhythmic Gamma Modulation. *Current Biology*, *25*(17), 2332–2337. https://doi.org/10.1016/j.cub.2015.07.048

Lisman, J., & Buzsaki, G. (2008). A Neural Coding Scheme Formed by the Combined Function of Gamma and Theta Oscillations. *Schizophrenia Bulletin*, *34*(5), 974–980. https://doi.org/10.1093/schbul/sbn060

Lisman, J. E., & Jensen, O. (2013). The Theta-Gamma Neural Code. *Neuron*, *77*(6), 1002–1016. https://doi.org/10.1016/j.neuron.2013.03.007

Lisman, J., & Idiart, M. (1995). Storage of 7 +/- 2 short-term memories in oscillatory subcycles. *Science*, *267*(5203), 1512–1515. https://doi.org/10.1126/science.7878473

Lövdén, M., Schmiedek, F., Kennedy, K. M., Rodrigue, K. M., Lindenberger, U., & Raz, N. (2013). Does variability in cognitive performance correlate with frontal brain volume? *NeuroImage*, *64*, 209–215. https://doi.org/10.1016/j.neuroimage.2012.09.039

MacDonald, S. W. S., Nyberg, L., & Bäckman, L. (2006). Intra-individual variability in behavior: links to brain structure, neurotransmission and neuronal activity. *Trends in Neurosciences*, *29*(8), 474–480. https://doi.org/10.1016/j.tins.2006.06.011

Maldonado, P. E. (2000). Dynamics of Striate Cortical Activity in the Alert Macaque: II. Fast Time Scale Synchronization. *Cerebral Cortex*, *10*(11), 1117–1131. https://doi.org/10.1093/cercor/10.11.1117

Miller, E. K., & Cohen, J. D. (2001). An Integrative Theory of Prefrontal Cortex Function. *Annual Review of Neuroscience*, *24*(1), 167–202. https://doi.org/10.1146/annurev.neuro.24.1.167

Pani, P., Di Bello, F., Brunamonti, E., D'Andrea, V., Papazachariadis, O., & Ferraina, S. (2014). Alpha- and beta-band oscillations subserve different processes in reactive control of limb movements. *Frontiers in Behavioral Neuroscience*, *8*. https://doi.org/10.3389/fnbeh.2014.00383

Python Core Team (2015). Python: A dynamic, open source programming language. Python Software Foundation. URL https://www.python.org/.

R Core Team (2014). R: A language and environment for statistical computing. R Foundation for Statistical Computing, Vienna, Austria. URL http://www.R-project.org/.

Schroeder, C. E., & Lakatos, P. (2009). Low-frequency neuronal oscillations as instruments of sensory selection. *Trends in Neurosciences*, *32*(1), 9–18. https://doi.org/10.1016/j.tins.2008.09.012

Senoussi, M., Verbeke, P., Talsma, D., & Verguts, T. (2018). Electrophysiological markers of instructed sensory-motor mappings: Testing a computational model of cognitive control. (November). San Diego, USA: Society for Neuroscience annual meeting.

Siegle, J. H., Pritchett, D. L., & Moore, C. I. (2014). Gamma-range synchronization of fast-spiking interneurons can enhance detection of tactile stimuli. *Nature Neuroscience*, *17*(10), 1371–1379. https://doi.org/10.1038/nn.3797

Solomon, E. A., Kragel, J. E., Sperling, M. R., Sharan, A., Worrell, G., Kucewicz, M., Inman, C. S., Lega, B., Davis, K. A., Stein, J. M., Jobst, B. C., Zaghloul, K. A., Sheth, S. A., Rizzuto, D. S., & Kahana, M. J. (2017). Widespread theta synchrony and high-frequency

desynchronization underlies enhanced cognition. *Nature Communications*, *8*(1). https://doi.org/10.1038/s41467-017-01763-2

Steegen, S., Tuerlinckx, F., & Vanpaemel, W. (2017). Using parameter space partitioning to evaluate a model's qualitative fit. *Psychonomic Bulletin & Review*, *24*(2), 617–631. https://doi.org/10.3758/s13423-016-1123-5

Storn, R., & Price, K. (1997). Differential Evolution - A simple and Efficient Heuristic for GLobal Optimization over COntinuous Spaces. *Journal of Global Optimization*, *11*(4), 341–359. https://doi.org/10.1023/A:1008202821328

Stroop, J. R. (1935). Studies of interference in serial verbal reactions. *Journal of Experimental Psychology*, *18*(6), 643–662. https://doi.org/doi:10.1037/h0054651

Usher, M., & McClelland, J. L. (2001). The time course of perceptual choice: The leaky, competing accumulator model. *Psychological Review*, *108*(3), 550–592. https://doi.org/10.1037//0033-295X.108.3.550

Verbeke, P., Ergo, K., De Loof, E., & Verguts, T. (2020). *Learning to synchronize: midfrontal theta dynamics during reversal learning* [Preprint]. Neuroscience. https://doi.org/10.1101/2020.06.01.127175

Verbeke, P., & Verguts, T. (2019). Learning to synchronize: How biological agents can couple neural task modules for dealing with the stability-plasticity dilemma. *PLOS Computational Biology*, *15*(8), e1006604. https://doi.org/10.1371/journal.pcbi.1006604

Verguts, T. (2017). Binding by Random Bursts: A Computational Model of Cognitive Control. *Journal of Cognitive Neuroscience*, *29*(6), 1103–1118. https://doi.org/10.1162/jocn_a_01117

Voloh, B., Valiante, T. A., Everling, S., & Womelsdorf, T. (2015). Theta–gamma coordination between anterior cingulate and prefrontal cortex indexes correct attention shifts. *Proceedings of the National Academy of Sciences*, *112*(27), 8457–8462. https://doi.org/10.1073/pnas.1500438112

Voloh, B., & Womelsdorf, T. (2016). A Role of Phase-Resetting in Coordinating Large Scale Neural Networks During Attention and Goal-Directed Behavior. *Frontiers in Systems Neuroscience*, *10*. https://doi.org/10.3389/fnsys.2016.00018

Wagenmakers, E.-J., Van Der Maas, H. L. J., & Grasman, R. P. P. P. (2007). An EZ-diffusion model for response time and accuracy. *Psychonomic Bulletin & Review*, *14*(1), 3–22. https://doi.org/10.3758/BF03194023

Zhou, T., Chen, L., & Aihara, K. (2005). Molecular Communication through Stochastic Synchronization Induced by Extracellular Fluctuations. *Physical Review Letters*, *95*(17). https://doi.org/10.1103/PhysRevLett.95.178103

i